The role of secondary data in estimating groundwater levels in the Iberian Peninsula

Nahed Ben-Salem[1,*], Amir Rouhani[1], Nadim K. Copty[2], Emmanouil A. Varouchakis[3], J. Jaime Gómez-Hernández[4], George P. Karatzas[5], Michael Rode[1,6], and Seifeddine Jomaa[1]

[1] Department of Aquatic Ecosystem Analysis and Management, Helmholtz Centre for Environmental Research - UFZ, Magdeburg, Germany (nahed.bensalem@outlook.com, amir.rouhani@ufz.de, michael.rode@ufz.de, seifeddine.jomaa@ufz.de),

[2] Institute of Environmental Sciences, Bogazici University, Istanbul, Türkiye (ncopty@bogazici.edu.tr),

[3] School of Mineral Resources Engineering, Technical University of Crete (TUC), Greece (varuhaki@mred.tuc.gr),

[4] Institute of Water and Environmental Engineering, Universitat Politècnica de València, Valencia, Spain (jaime@dihma.upv.es),

[5] School of Chemical and Environmental Engineering, Technical University of Crete (TUC), Greece (karatzas@mred.tuc.gr),

[6] Institute for Environmental Science and Geography, University of Potsdam, Potsdam, Germany.

Published in ***Groundwater for Sustainable Development***. Volume 33, May 2026, 101594,
https://doi.org/10.1016/j.gsd.2026.101594

[*]Corresponding Author: Nahed Ben-Salem (nahed.bensalem@outlook.com)

Abstract

Mapping groundwater levels at the regional scale is often hindered by the lack of high-density direct head measurements. In this study, we explore the value of incorporating different secondary data with cokriging to assess the spatial variability of groundwater levels for the entire Iberian Peninsula, a region characterized by pronounced hydroclimatic variability and rising water demand. The analysis uses more than 60 years of groundwater level measurements from 3,822 observation wells across the region, combined with readily available secondary data, including a digital elevation model, precipitation data, and hydrogeological information. Because of the time series length, the analysis was divided into four periods, each containing a different number of measurements. The performance of the geostatistical models was rigorously evaluated through cross-validation and statistical metrics. Results showed that for earlier periods, characterized by a limited number of observation wells, incorporating groundwater data from subsequent periods and hydrogeological information led to the most significant improvement in groundwater level mapping. Average annual precipitation data did not correlate with groundwater level data and had minimal impact on the interpolation, whereas digital elevation models had a mixed effect. Overall, the study underlines the value of incorporating secondary data through cokriging to map groundwater levels at a regional scale when in-situ data are scarce.

Keywords

Multi-decadal analysis, kriging, cokriging, groundwater level, geostatistics, spatial variability, Iberian Peninsula.

Highlights

- Long-term average groundwater levels mapped for the Iberian Peninsula.
- Value of various secondary data (DEM, precipitation, groundwater level) is examined.
- Hydrogeological context increased the reliability of groundwater head maps.
- Annual precipitation showed a weak relation to groundwater level patterns.

1. Introduction

Groundwater is a crucial component of the global water cycle, serving as a fundamental source of water for irrigation, domestic use, and ecosystem services (Rohde et al., 2024). Groundwater resources act as natural water reserves that mitigate seasonal and long-term water stress. Groundwater supports agriculture and ensures sustainable crop production, especially in arid and semi-arid regions (Famiglietti, 2014). At the same time, it contributes to the conservation of ecosystems by maintaining groundwater discharges into wetlands and rivers, thus helping to preserve habitats and biodiversity (Erostate et al., 2020).

Increasing human-induced impacts on climate and the water cycle have significantly affected surface water, groundwater recharge, and sustainability (de Marsily, 2021). The overexploitation of aquifers can significantly reduce groundwater yield, altering groundwater flow patterns and leading to water quality deterioration, e.g., seawater intrusion in coastal regions (Xiao, 2021). The decline in groundwater levels also affects groundwater-dependent ecosystems (Erostate et al., 2020) and threatens food security (Moench et al., 2009; Gelati et al., 2020).

Groundwater levels are subject to short-term, seasonal, and long-term fluctuations due to natural variations and anthropogenic pressures. Long-term and frequent monitoring of groundwater levels is essential for assessing the availability of groundwater resources under dynamic conditions. Analyzing multi-decadal trends in groundwater levels is fundamental for effective water resource management and planning (Dahlke et al., 2018; Ma et al., 2017). Long-term trends in groundwater levels provide useful insights into historical variations and help in understanding hydrological changes over time (Power et al., 1999; Chávez García Silva et al., 2024), including potential threats to ecosystems' biodiversity and water availability (Huggins et al., 2023).

This study addresses decadal-average groundwater conditions, which smooth seasonal and multi-year variability to highlight long-term regional patterns. Short-term fluctuations are therefore beyond the scope of this analysis. Groundwater levels are expressed relative to mean sea level, which is the standard reporting format across Iberian datasets and enables consistent regional interpolation. We note, however, that depth to groundwater below land surface is often more relevant for ecological and management applications, and this remains an important direction for future work. As conventional direct groundwater monitoring remains inconsistent, patchy, and scarce, groundwater measurements are generally only possible at limited locations. Previous studies have used various interpolation algorithms, mainly geostatistical methods, which have been considerably refined over time to determine groundwater levels' spatial and temporal variability (Ahmadi and Sedghamiz, 2007; Cay and Uyan, 2009). To address the issue of data scarcity, some studies have incorporated related secondary data that are more readily available (Asante et al., 2022). In cokriging, secondary data such as topographical, geological, climatic, or remotely sensed data can serve as auxiliary information to enhance the spatial prediction of groundwater attributes when primary data are sparse (e.g., Ahmed and de Marsily, 1987; He et al., 2014; Ravish et al., 2025). These secondary datasets, often easier and more cost-effective to obtain, help refine interpolation models and reduce prediction uncertainty. By leveraging such multi-source data integration, cokriging has proven to be a valuable geostatistical approach for improving groundwater resource assessment, particularly in regions with limited direct observations.

Although numerous data-interpolation techniques have been developed over the past decades, studies that specifically focused on predicting groundwater levels over multi-decadal periods and on a large scale are relatively few (Huang et al., 2015; Gong et al., 2018), underscoring the need for more long-term studies (Dahlke et al., 2018). The lack of long-term data covering a large domain and the hydrogeological complexity of subsurface systems are key impediments to multi-decadal groundwater level assessments.

The purpose of this study is to establish a regional-scale, long-term characterization of groundwater levels across the Iberian Peninsula using different secondary datasets, including precipitation, DEM, average groundwater level, and hydrogeological units. This regional perspective is designed to reveal large-scale groundwater patterns and spatial variability rather than local dynamics. By combining in-situ groundwater observations with multiple secondary datasets, our study provides a reference framework that complements both site-specific analyses and process-based models, while also identifying the limitations imposed by data density and temporal averaging.

Groundwater levels are controlled by a combination of recharge, discharge, aquifer geometry, and subsurface hydraulic properties. At broad regional scales, topography (expressed through DEM) influences groundwater gradients and flow directions, as water tables tend to align with equipotential contours related to surface elevation (Tóth, 1963; Refsgaard et al., 2021). Precipitation governs the long-term replenishment of aquifers, especially in Mediterranean and semi-arid climates, where interannual variability can dominate recharge dynamics (Tularam and Keeler, 2024). Hydrogeological descriptors (e.g., aquifer type, lithology) further modulate how recharge translates into groundwater head changes, as different lithologies exhibit distinct storage and transmissivity characteristics. The combined use of these secondary variables in a spatial interpolation framework is conceptually justified insofar as they serve as proxies for the dominant physical controls on groundwater distribution at continental and regional scales. The main objective of this study is to investigate the multi-decadal spatial variability of groundwater levels across the Iberian Peninsula and to assess the benefit of using secondary data in the interpolation. The specific objectives are (i) to analyse the multi-decadal changes and spatial patterns of groundwater levels in the Iberian Peninsula, (ii) to develop groundwater level maps using cokriging with different secondary data, including precipitation, digital elevation models, and hydrogeological properties, and (iii) to evaluate the benefit of including the different secondary data in the interpolation of groundwater levels at regional scale using cross-validation method. The Iberian Peninsula, with its long-term in situ monitoring data, well-

characterized subsurface heterogeneity, and strong dependence on groundwater resources, represents a unique large-scale demonstration site for assessing the capability of cokriging with different secondary data in evaluating multi-decadal groundwater level changes.

2. Materials and methods

2.1. Research area

The Iberian Peninsula, located in southwestern Europe, covers an area of approximately 583,000 km². Its landscape is characterized by complex orography, with inland plateaus bordered by mountain ranges that, in some areas, extend to the coast. The region has a Mediterranean climate with a long dry season in which evapotranspiration is largely controlled by water availability. Precipitation patterns are becoming more seasonal, and there is an increased interaction between land and atmosphere (Rios-Entenza et al., 2014). The Cantabrian Mountains, which receive about 700 mm of precipitation annually (Font Tullot, 2000; Rodríguez-Rodríguez et al., 2015), separate the humid northwest from the rest of the peninsula. The north-western highlands record the highest average annual precipitation, exceeding 2800 mm, making them among the wettest areas in Europe (Cardoso et al., 2013). In contrast, the southeast is the driest region, with annual precipitation below 200 mm, the lowest in Europe (Font Tullot, 2000). Much of the eastern and central Iberian Peninsula has a semi-arid climate (Gimeno et al., 2010; Pérez and García, 2023). Along the Mediterranean coast, precipitation peaks in fall (Millán et al., 2005), while inland areas without maritime influence receive significant precipitation in spring, which is crucial for agriculture and plant ecosystems. Summers tend to be dry. In recent decades, groundwater use for irrigation has increased dramatically in the arid and semi-arid regions of Spain, following a trend observed in many Mediterranean regions and elsewhere. However, irrigation is often carried out by farmers without sufficient supervision or planning by the water management authorities (Garrido et al., 2006; Portoghese et al., 2025). The Iberian Peninsula exhibits diverse hydrogeological conditions due to its varied climate and geology. The northern and north-western regions are dominated by alluvial and fractured bedrock aquifers, which benefit from high

precipitation and provide significant groundwater recharge (Martínez-de la Torre and Miguez-Macho, 2019). In contrast, the southern and south-eastern regions are more arid, with karstic aquifers that offer limited but crucial groundwater resources (Martín-Rodríguez et al., 2023). The central and eastern areas are characterized by sandstone and conglomerate aquifers, which vary in recharge depending on seasonal rainfall (Diodato et al., 2024). Overall, groundwater availability is highly influenced by regional climate and geology, with sustainability concerns in areas facing low recharge and high abstraction.

2.2. Data used in analysis

Groundwater level monitoring data in the Iberian Peninsula extend back to the 1960s. To examine the evolution of groundwater levels, we divided the data into four periods: (a) 1965-1984 (20 years), (b) 1985-1994 (10 years), (c) 1995-2004 (10 years), and (d) 2005-2020 (15 years). The first column of Fig. 1 shows the spatial distribution of the groundwater observation points and their time-averaged groundwater levels across the Iberian Peninsula for each period.

These periods were specifically chosen to capture distinct phases of climatic, hydrological, and anthropogenic change in the Iberian Peninsula, rather than using equal time intervals. The unequal period lengths reflect data availability constraints and the need to align with significant environmental and management transitions. The initial period (1965-1984) encompasses the early monitoring phase when wells were scarce, particularly in the western half of the peninsula, while the second period (1985-1994) captures the initial expansion of monitoring networks, though wells remained concentrated in the eastern region. These two periods (1965-1984 and 1985-1994) represent relatively stable groundwater conditions before the sharp increase in reliance on groundwater extraction for irrigation (Custodio, 2002).

The latter two periods (1995-2004 and 2005-2020) correspond to marked changes in precipitation patterns (López-Moreno et al., 2010; Miró et al., 2023) and significant increases in groundwater reliance for domestic and irrigation purposes. Both periods show continued expansion of monitoring wells, though

158 spatial concentration in the eastern peninsula persists. This approach allows for a more spatiotemporally

159 focused and robust analysis of groundwater evolution patterns.

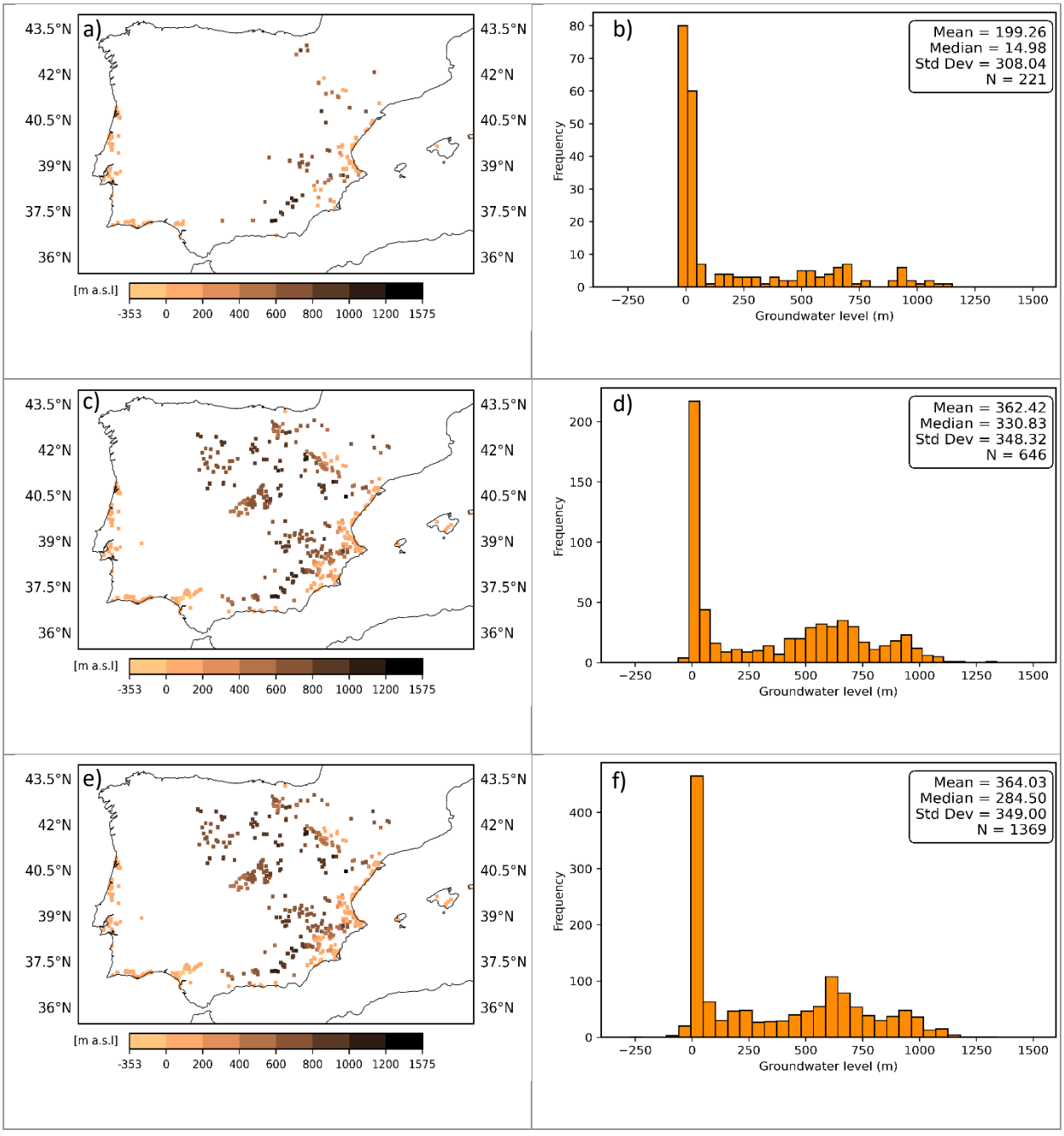

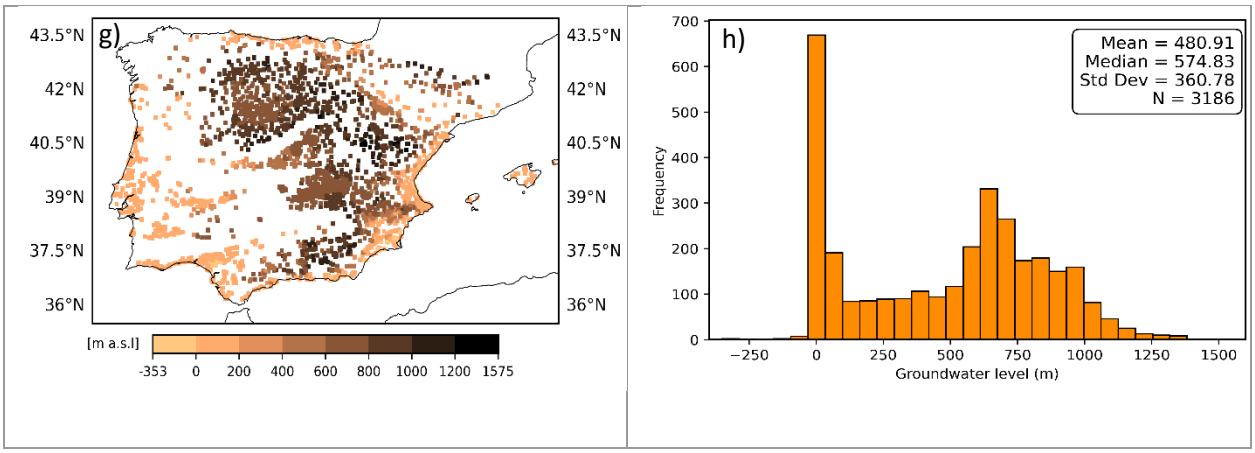

160 **Fig. 1.** Spatial distribution of time-averaged groundwater levels (m a.s.l.) in the Iberian Peninsula (left
161 column) and corresponding histograms (right column) over four periods: (a, b) 1965–1984, (c, d) 1985–
162 1994, (e, f) 1995–2004, and (g, h) 2005–2020.

163 Fig. 2 shows the secondary datasets considered in the interpolation of the groundwater level, including (i)
164 digital elevation models (DEM) derived from the Shuttle Radar Topography Mission (SRTM) with
165 approximately 30 m resolution; (ii) average groundwater level data for the entire period: 1965-2020 at the
166 3822 groundwater level monitoring wells, estimated using the arithmetic mean of all available
167 measurements at that location; (iii) average annual precipitation data over the entire Iberian Peninsula,
168 obtained from the gridded (0.1° resolution) dataset of precipitation for the period 1971-2015 (Herrera et
169 al. (2019); and (iv) hydrogeological maps of the entire study area, obtained from the Spanish Geological
170 Survey (https://info.igme.es/cartografiadigital/Tematica/Default.aspx?language=en, last accessed June 10,
171 2025). The 3822 monitoring wells include 2883 wells in Spain and 939 in Portugal. Groundwater level data
172 for Spain (1965–2017) were obtained from the Ministry of Agriculture and Fisheries, Food and
173 Environment, and the Ministry of Ecological Transition, through the Monitoring Network Information
174 System Portal
175 (https://www.mapama.gob.es/app/descargas/descargafichero.aspx?f=basedatospiezometria.zip, last
176 accessed June 10, 2025). Groundwater data for Portugal (1980–2020) were obtained from the Portuguese

177 Environmental Agency through the National Water Resources Information System (SNIRH)
178 (https://snirh.apambiente.pt/, last accessed September 22, 2021).
179 All data used in this study were pre-processed and checked to ensure the reliability and integrity of the
180 gathered data. Groundwater well data, which are point-based measurements, were inspected for missing
181 values, duplicates, and outliers, and then re-projected to the World Geodetic System (WGS) 1984 (EPSG:
182 4326). The DEM was re-gridded to the same 4 km × 4 km resolution as the interpolated groundwater
183 dataset, ensuring consistency between topographic and groundwater levels. This resolution reflects the
184 effective spacing of the data rather than the minimum borehole distance. Precipitation data were sourced
185 from the Iberia 1.0 gridded dataset (0.1° resolution, 1971-2015), aggregated into annual means. These
186 were interpolated using Inverse Distance Weighting (IDW) due to its computational efficiency in handling
187 densely sampled climate data, which aligns with other spatial layers. Given the data's gridded nature and
188 regional scale, further geostatistical interpolation (e.g., kriging) was not required. Interpolation of
189 groundwater levels was performed at a 4 km × 4 km grid, representing regional piezometric heads rather
190 than individual well measurements. The 'regional scale' refers to the Iberian Peninsula and its major
191 hydrogeological units. Local influences, such as pumping or land-use changes, were not directly accounted
192 for due to the use of decadal averages and the coarse grid, but were indirectly captured through their
193 effects on long-term trends. Hydrogeological units were grouped into four categories based on lithology
194 and aquifer properties. As the groundwater level time series length varied, time averages for each period
195 were used in all interpolations. These pre-processing steps ensured consistency and compatibility for
196 groundwater analysis.
197 Prior to variogram and cokriging analysis, groundwater levels and secondary variables were examined for
198 differences in scale, units, and distributional properties. No standardization or nonlinear transformation
199 was applied, as exploratory analysis indicated that the spatial structure was adequately captured in the
200 original physical units. Variogram-based geostatistical methods, including cokriging, estimate spatial

dependence through experimental variograms and cross-variograms without requiring prior rescaling of variables when units and ranges are consistent with model assumptions, and this approach is commonly adopted in regional spatial studies (Giraldo et al., 2023; Dowd and Pardo-Igúzquiza, 2024). All groundwater level maps are therefore presented directly in physical units.

2.3. Spatial interpolation procedure

The separation distance between observation wells is variable (see Fig. 1), with some wells located hundreds of meters apart. The spatial interpolation of groundwater levels was performed for each period (1965-1984, 1985-1994, 1995-2004, and 2005-2020) using different kriging approaches. All interpolations were conducted on a common 4 km × 4 km grid, allowing direct temporal comparison. Cokriging was performed without detrending to retain the low-frequency spatial variability inherent in the data, as detrending can remove meaningful large-scale patterns and impose model-dependent biases that may compromise the integrity of the variogram and subsequent spatial predictions.

As a baseline scenario, groundwater levels were first interpolated using simple kriging without secondary variables for each temporal period. This baseline provided a direct reference against which the effect of incorporating secondary datasets through cokriging was assessed. Simple kriging and cokriging were implemented on the same 4 km × 4 km grid and evaluated using identical cross-validation procedures. This consistent framework ensures that differences in performance are attributable to the inclusion of secondary information rather than differences in model configuration or validation strategy (Hengl et al., 2018; Zimmerman et al., 2020).

Temporal non-stationarity in groundwater observations may arise from long-term changes in climate forcing, land use, and groundwater abstraction, particularly when multi-decadal datasets are analysed. To address this issue, the dataset was stratified into four temporal periods, and experimental variograms and

cross-variograms were computed independently for each period. This allowed an assessment of the stability of spatial correlation structures through time.

Comparisons across periods indicate that while some variability in variogram parameters (notably sill and range) exists (Table 1), the overall variogram shapes and model families remain broadly consistent. These differences are partly attributable to variations in the number and spatial distribution of observations across periods, which affect variogram reliability, particularly at larger lag distances. Given this context, a common variogram model form was retained, with period-specific parameterization, ensuring internal consistency while accommodating temporal non-stationarity within each period. All experimental variograms and cross-variograms are provided in the Supplementary Information to document this assessment.

The full observation period (1965–2020) was subdivided into four temporal intervals (1965–1984, 1985–1994, 1995–2004, and 2005–2020). This segmentation was defined based on a combination of data availability, spatial density of monitoring wells, and consistency of measurement frequency. Earlier periods are characterized by sparse and irregular monitoring, whereas later periods exhibit increased station density and improved temporal coverage. The selected intervals, therefore, represent a compromise between temporal resolution and spatial representativeness, ensuring sufficient observations within each period to support robust geostatistical modelling while preserving long-term groundwater evolution signals.

For the first two periods (1965-1984 and 1985-1994), which are characterized by a relatively small number of wells, four different interpolation approaches were applied: (1) simple kriging using only groundwater level data, (2) cokriging with DEM as a secondary data, (3) cokriging with precipitation as a secondary data, and (4) cokriging with the average groundwater level for the entire period (1965-2020) as a secondary data.

245 The average groundwater level filters out short-term variations, while the DEM and precipitation data
246 reveal the impact of elevation and climate on the groundwater level distribution.
247 For the third and fourth periods (1995-2004 and 2005-2020), which have higher data density, three
248 different interpolation approaches were used: (1) cokriging with DEM as a secondary data, (2) cokriging
249 with precipitation as a secondary data, and (3) simple kriging performed separately on each hydrogeological
250 unit whereby groundwater wells were first subdivided based on their location within identified
251 hydrogeological units. Subsequently, simple kriging was applied independently to each unit with variograms
252 and means recomputed separately.
253 For each unit and period, variograms were computed from the data, and exponential models were fitted
254 to represent the spatial correlation structure. The interpolation was performed separately for each unit,
255 and the resulting interpolated surfaces were subsequently merged to produce a composite groundwater
256 level map. In some cases, the correlation ranges exceeded the size of individual units, reflecting regional-
257 scale groundwater flow systems. Groundwater head data were obtained from in-situ measurements
258 collected at monitoring wells distributed across the study area. Interpolation was carried out within each
259 hydrogeological unit, and areas outside the corresponding unit boundaries were masked to avoid cross-
260 unit extrapolation. All observed groundwater levels were incorporated in the kriging interpolation scheme,
261 which does not explicitly consider the depth of the screened interval of the well or the potential presence
262 of multiple aquifer systems. For all periods and cases, spatial interpolation was performed using the ArcGIS
263 geostatistical analysis tool (ESRI, 2023). This tool first estimates the groundwater level variogram and its
264 cross-variogram with secondary data and then performs the interpolation.
265 Cokriging relies on the assumption of second-order stationarity of both the primary and secondary variables
266 within the domain of analysis. In long-term groundwater datasets, this assumption may be violated when
267 observations influenced by contrasting climatic or anthropogenic conditions are pooled together (Bierkens
268 and Wada, 2023). In this study, temporal stationarity across periods is therefore not assumed. Cokriging is

applied independently within each predefined temporal interval, using period-specific covariance and cross-covariance structures, to ensure that spatial dependence is characterized under relatively stable hydro-climatic conditions. Within each period, groundwater observations are temporally aggregated to represent mean conditions, which serves to attenuate short-term fluctuations related to seasonal variability or episodic recharge events. Temporal aggregation is commonly adopted in large-scale groundwater assessments to enhance the robustness of spatial relationships when the objective is regional mapping rather than short-term dynamics (Zhang and Schaap, 2019).

Groundwater levels were interpolated using simple kriging, which assumes a known and constant mean within each temporally segmented period. In this study, period-specific mean groundwater levels were estimated from the observations, while spatial variability was represented through the covariance structure. This approach yields statistically optimal predictions when the mean is reasonably approximated and enables consistent uncertainty estimation across large and heterogeneous regions (Wackernagel, 2003; Webster and Oliver, 2007).

Model robustness was assessed through leave-one-out cross-validation performed independently for each temporal period. By predicting groundwater levels at observation locations excluded from the interpolation, this procedure provides an effective evaluation of model stability under data perturbation. In large-scale geostatistical applications, cross-validation is widely used as a practical and statistically sound alternative to formal sensitivity analyses, particularly when data availability and computational constraints limit extensive scenario testing (Olea, 2009).

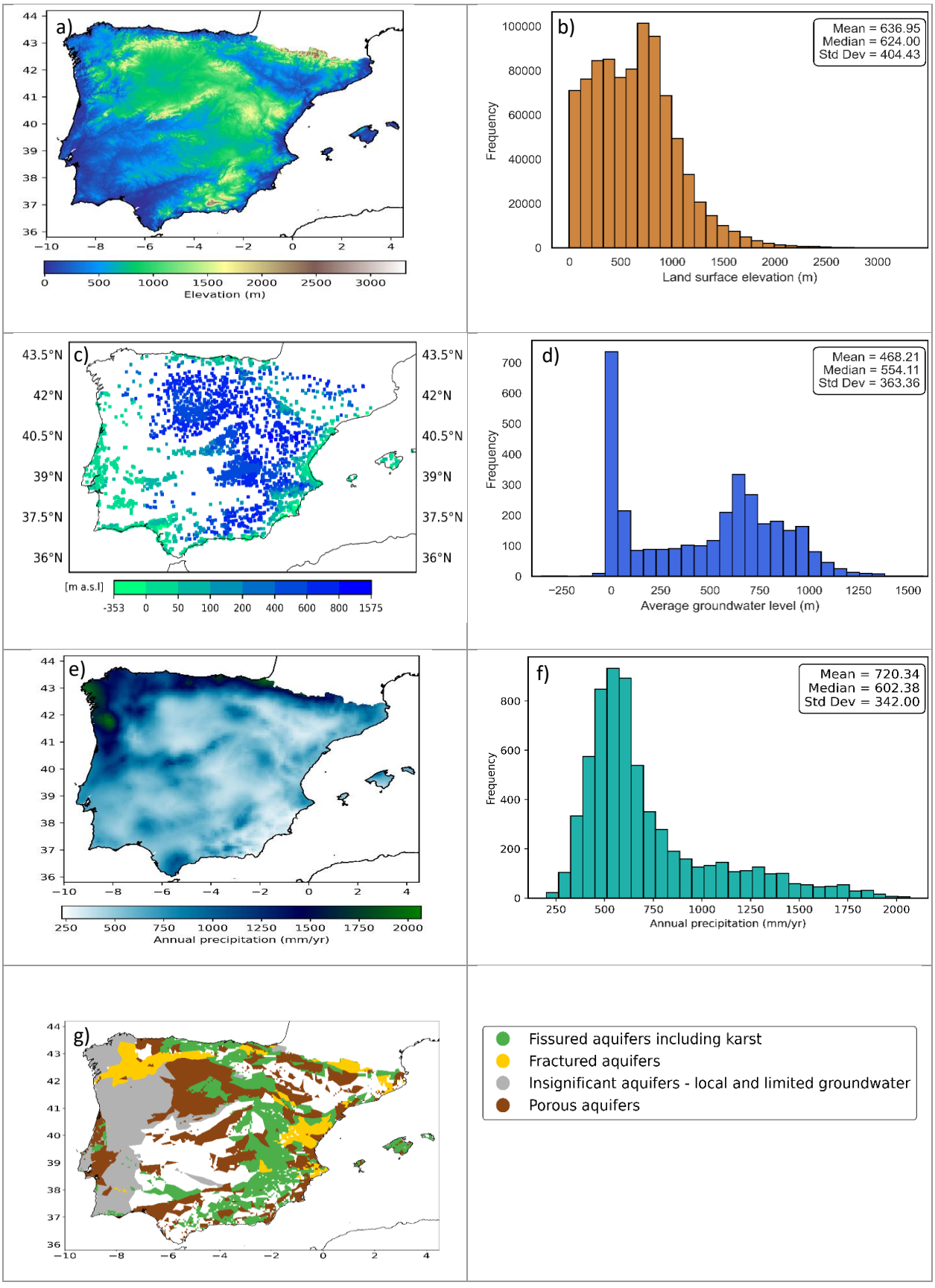
a)
Elevation (m)
b)
Mean = 636.95
Median = 624.00
Std Dev = 404.43
Frequency
Land surface elevation (m)
c)
[m a.s.l]
d)
Mean = 468.21
Median = 554.11
Std Dev = 363.36
Frequency
Average groundwater level (m)
e)
Annual precipitation (mm/yr)
f)
Mean = 720.34
Median = 602.38
Std Dev = 342.00
Frequency
Annual precipitation (mm/yr)
g)
Fissured aquifers including karst
Fractured aquifers
Insignificant aquifers - local and limited groundwater
Porous aquifers

Fig. 2. Secondary data used in this study (left column) and their corresponding histograms (right column): (a, b) land surface elevation, (c, d) average groundwater level for the full period (1965–2020), and (e, f) average annual precipitation. Geological units (g) were used to guide the interpolation of groundwater levels for the third and fourth periods. Note: White areas denote zones outside the spatial domain of the hydrogeological unit used for interpolation. These regions were excluded a priori to prevent interpolation across non-contiguous geological units.

2.4. Performance criteria

We employed a leave-one-out cross-validation approach to evaluate the predictive performance of the interpolation methods applied to groundwater level data (Goovaerts, 1997; Allard et al., 2013). In this procedure, each observation is successively removed from the dataset, and its value is predicted using the remaining data. This yields a set of predicted values that can be directly compared with the corresponding observed values at the same locations.

Two standard validation metrics were used to assess model performance across the four analysis periods: the root mean square error (RMSE), which measures the overall magnitude of prediction errors, and the mean error (ME), which quantifies systematic bias in the predictions. The error metrics were calculated as follows:

$$RMSE = \sqrt{\sum_{i=1}^{n}\left(\hat{\mathrm{Z}}(\mathrm{x}_i) - \mathrm{Z}(\mathrm{x}_i)\right)^2/n} \quad (1)$$

$$ME = \frac{\sum_{i=1}^{n}(\hat{\mathrm{Z}}(\mathrm{x}_i) - Z(\mathrm{x}_i))}{n} \quad (2)$$

where n is the number of locations where the cross-validation was performed, $Z(x_i)$ is the observed value of Z at location (x_i), and $\hat{Z}(x_i)$ is the predicted value at the same location.

309 In addition to these error metrics, we examined co-kriging variance maps as a measure of the uncertainty
310 associated with the spatial interpolation. These variance maps reflect the estimation uncertainty values at
311 each location and are influenced by the spatial distribution of observations and the fitted variogram or
312 cross-variogram models. All interpolation procedures were performed using the Geostatistical Analyst
313 extension in ArcGIS Pro 3.1 (ESRI, 2023). Model results and uncertainty maps were further processed and
314 visualized using Python-based tools.

315 Semi-variograms and cross-covariances were calculated empirically and modelled using exponential
316 functions, which consistently provided a good fit to the data, capturing both short- and long-range spatial
317 continuity. Variogram modelling was carried out separately for each variable and period before evaluating
318 the models' predictive performance.
319 Interpolation performance was evaluated using standard descriptive validation metrics, including root
320 mean square error and mean error, computed through cross-validation. Differences between interpolation
321 approaches are interpreted in a comparative rather than inferential sense. Formal statistical significance
322 testing was not performed, as cross-validation errors are spatially dependent and therefore violate the
323 independence assumptions required for classical hypothesis testing. This descriptive evaluation framework
324 is commonly adopted in spatial prediction studies, particularly at large scales where the primary objective
325 is model comparison rather than formal inference (Brus et al., 2011; Zimmerman, 2006).

326 ## 3. Results

327 This section presents the results of the interpolation methods used to estimate groundwater levels in the
328 Iberian Peninsula. First, the correlation of the groundwater level with each of the secondary data is
329 presented. This is followed by a histogram of each variable, along with the estimated variograms and cross-
330 variograms for each period. The interpolation results are presented in the form of groundwater level maps.

The performance of each interpolation scheme is evaluated in terms of the error metrics and kriging variance maps (Table 1).

3.1. Correlation of groundwater level data to the secondary data

Fig. 3 shows scatter plots of the observed groundwater level against land surface elevation, precipitation, and average groundwater level for each of the four time periods. All groundwater levels were referenced to mean sea level. Consequently, in some elevated terrains with excessive extraction, the water table may occur below the mean sea level, resulting in negative groundwater levels.

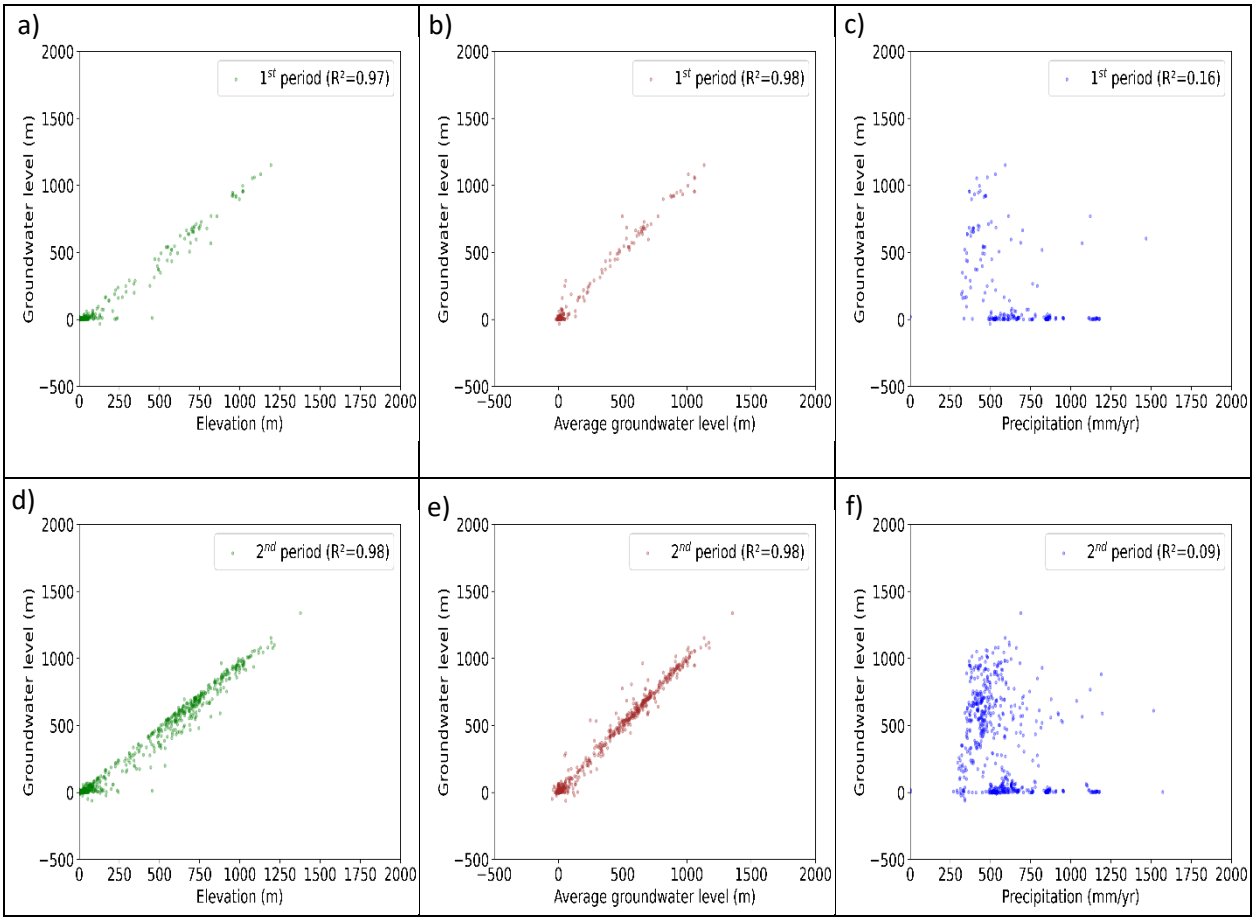

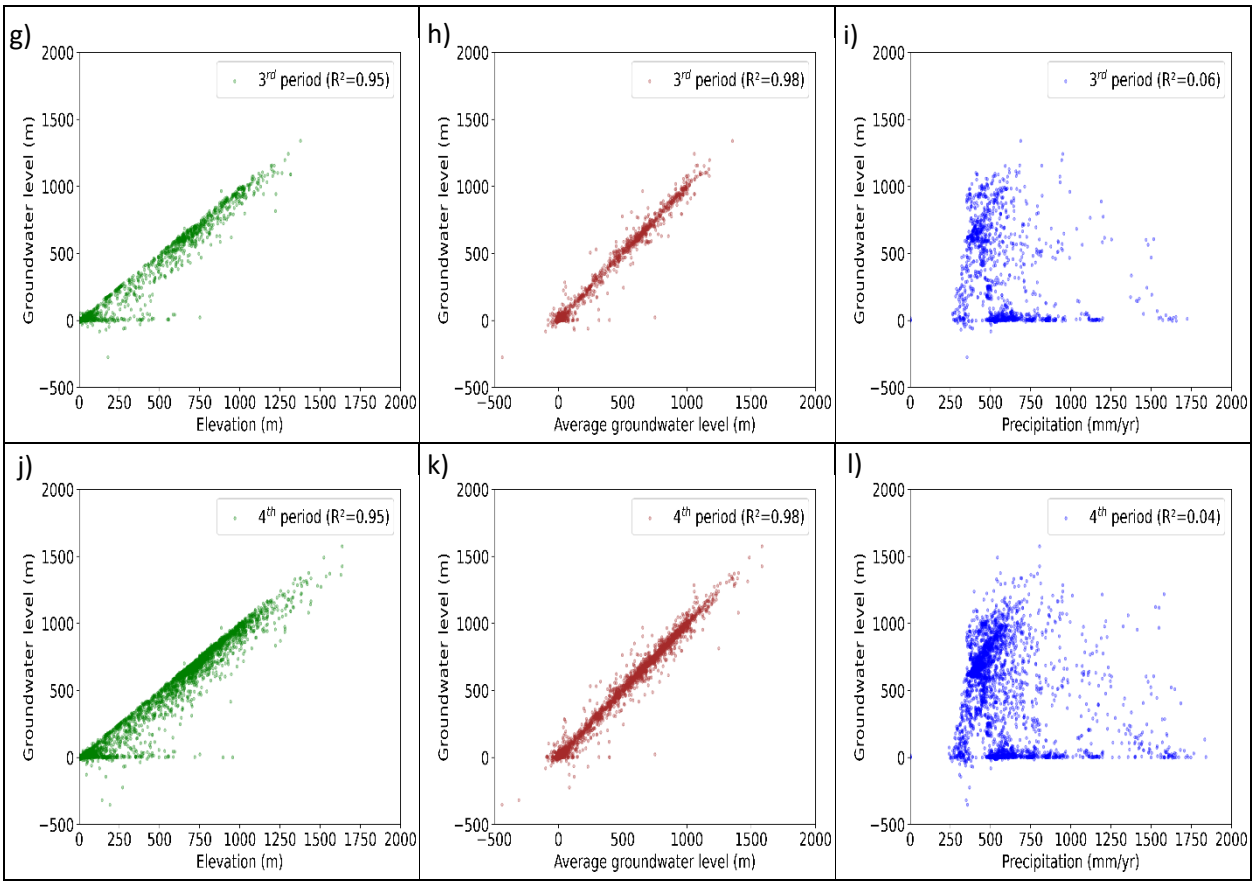

Fig. 3. Scatter plots of observed groundwater levels for periods one to four against the digital elevation models (DEM) (column 1: a, d, g, j), the time-averaged groundwater level (column 2: b, e, h, k), and annual precipitation (column 3: c, f, i, l). Note: Groundwater levels are expressed relative to mean sea level. Negative values in upland areas reflect deep water tables below the ground surface and do not indicate erroneous measurements.

Across the four periods, there was a robust positive correlation between groundwater levels and DEM, suggesting a significant influence of topography on groundwater distribution patterns. This correlation persisted as the data points increased in subsequent periods. The correlation between groundwater levels and DEM resulted in coefficients of determination R^2 between 0.95 and 0.97. Inspection of the scatterplots shows that high-elevation areas in the Iberian Peninsula tend to have high groundwater levels, while this relationship is not as strong for low-elevation areas. This is consistent with previous studies that have

shown a significant relationship between DEM and groundwater in the Mediterranean region, where geographical characteristics are considered the main factors of groundwater recharge (Muhs, 2020; Ruiz et al., 2023; Somers and McKenzie, 2020).

A significant correlation was found between the observed groundwater levels of the four different periods and the average groundwater levels. This correlation is expected to exist given the relatively steady groundwater levels within the study area. The strong correlation (R^2 = 0.98 for all four periods) between observed groundwater levels and average groundwater levels suggests that groundwater levels are relatively stable over the long term and are not significantly affected by short-term fluctuations due to climatic conditions or other anthropogenic factors.

No significant correlation was observed between groundwater levels and annual precipitation for the four studied periods. This result indicates that annual precipitation variations are not an important factor influencing groundwater level fluctuations directly. The statistically insignificant correlation could be due to the highly variable precipitation and the fact that groundwater recharge is influenced by various complex factors, including soil permeability, hydrogeology, aquifer characteristics, and local hydrological processes (Manna et al., 2019; Lorenzo-Lacruz et al., 2017). This lack of correlation can also be attributed to the delayed response of groundwater systems to precipitation events, as groundwater levels generally reflect longer-term hydrological processes rather than current weather conditions (Hellwig et al., 2020; Liu et al., 2023). While a delayed correlation between precipitation and piezometric heads may exist when analyzed at shorter time intervals, such an analysis was not conducted here due to the unavailability of higher-frequency data.

3.2. Histograms and cross-variograms of the groundwater level and secondary data

The histograms of the primary variable (groundwater levels) and the secondary data (DEM, precipitation, and average groundwater levels) exhibit distinct statistical and spatial characteristics across the four periods. Groundwater level histograms consistently showed a bimodal distribution, indicating the presence of two dominant hydrogeological regimes. Precipitation displayed moderate positive skewness, reflecting occasional extreme precipitation events, while DEM values followed a near-normal distribution, consistent with the region's relatively stable topographic gradients. Table 1 summarizes the fitted model parameters, while the corresponding raw and modelled variograms and cross-variograms are provided in the supplementary material (Figs. S1-S3).

The histograms in Fig. 1 show the frequency distribution of time-averaged groundwater levels for each period considered. Across all four periods, the distributions exhibit a consistent bimodal distribution, indicating the presence of two dominant groundwater level ranges. This bimodality likely reflects the spatial heterogeneity of the Iberian Peninsula, particularly the contrast between low-lying sedimentary basins and higher-altitude or mountainous regions. The persistence of this pattern over time suggests that these hydrogeological features exert a stable control on the regional groundwater distribution.

Experimental variograms of groundwater levels were computed separately for each temporal period using omnidirectional lags to characterize large-scale spatial dependence. Spherical, exponential, and Gaussian models were tested, and the final model was selected based on visual agreement with the empirical variogram and reduced residual structure at short to intermediate lags, consistent with common practice in regional-scale studies (Chilès and Delfiner, 2012). Cross-variograms between groundwater levels and secondary variables were modeled using the same functional form within a linear model of coregionalization, ensuring positive definiteness and consistency between direct and cross-covariance structures (Wackernagel, 2003).

392 Directional variograms were explored to assess potential anisotropy associated with large-scale
393 groundwater flow patterns or regional geological structures. No persistent or systematic anisotropy was
394 identified at the scale of the Iberian Peninsula. Consequently, isotropic variogram models were retained to
395 avoid over-parameterization and to enhance robustness given the heterogeneous spatial distribution of
396 monitoring wells.

397 Experimental variograms and cross-variograms were computed for each period separately. For the last two
398 periods, they were also computed independently for each hydrological unit. Raw semi-variograms and
399 cross-covariances were computed separately for each period using a 12-lag distance and 30 bins. The
400 analysis revealed a weak anisotropic structure, with some variograms and covariance functions showing
401 greater spatial continuity in the north-south direction than in the east-west direction. This suggests a
402 preferential groundwater flow or structural influence along the north-south axis. However, given that the
403 anisotropy was not sufficiently pronounced, isotropic modelling was adopted in all cokriging schemes.

404 For the first and second periods, the cross-covariances were computed between the secondary data DEM
405 and precipitation on one hand and the average groundwater levels. The cross-variograms show a very weak
406 correlation between groundwater levels and precipitation. In contrast, DEM exhibited a more stable, long-
407 range correlation with groundwater levels.

408 For the third and fourth periods, because the correlation between the precipitation and groundwater level
409 data was weak, precipitation was discarded, and only the groundwater levels and DEM were used as
410 secondary data. In addition, given that the amount of data was much larger than for the other two periods,
411 it was possible to segment the data by hydrogeological unit and perform a simple kriging analysis of
412 piezometric heads per hydrogeological unit without accounting for any secondary variable.

413 **Table 1.** Statistical metrics of the best-fit correlation function of groundwater levels and secondary data for

414 each period.

Period	Data type	Variable	Nugget	Sill	Range[1] (km)
First period (1965-1984)	SV	-	0.027	0.864	812
	SV	Average GW	0.023	0.432	529
	SV	DEM	0.024	0.478	573
	SV	Precipitation	0.027	-0.476	647
Second period (1985-1994)	SV	-	0	1.321	722
	SV	Average GW	0	0.776	435
	SV	DEM	0	0.932	433
	SV	Precipitation	0	-0.394	517
Third period (1995-2004)	SV	DEM	0.003	0.823	446
	HU	Fissured	0	1.004	244
	HU	Fractured	0	1.122	73
	HU	Insignificant	0.153	0.4	33
	HU	Porous	0.03	1.15	632
Fourth period (2005-2020)	SV	DEM	0	0.741	401
	HU	Fissured	0	1.012	333
	HU	Fractured	0	1.087	151
	HU	Insignificant	0.036	0.802	358
	HU	Porous	0	0.810	491

415 *SV: secondary variable, HU: hydrogeological unit, Average GW: average groundwater level, DEM: Digital Elevation

416 Model. [1] Range is defined as three times the integral scale.

417 The nugget and sill values of the fitted variograms are reported separately. In most cases, the nugget is

418 small or negligible, indicating low short-range variability and suggesting that the spatial structure is well

419 captured even at the smallest lag distances. The sill represents the total variance (for direct variograms) or

420 cross-covariance (for cross-variograms) between variables. However, in cases where a nugget effect is

421 present, such as for precipitation, the higher nugget-to-sill ratio suggests short-range variability and

422 potential local influences. The fitted model parameters, including nugget, sill, and range, are detailed in

423 Table 1, and the raw versus modelled functions are illustrated in Figs. S1-S3.

424 It is observed that the correlation length scales (range) of the best-fit variograms are generally on the order

425 of several hundred km up to about 800 km. This broadly correlates with the typical size of aquifer systems.

426 Moreover, the correlation length scale in porous aquifer systems, which are the most exploited aquifers,
427 seems to be larger than that of other aquifer systems.

428 The cross-covariance analysis provided further insight into the relationship between groundwater levels
429 and secondary data. Notably, annual precipitation exhibited a weak spatial correlation with groundwater
430 levels, as also revealed by the scatter plots (Fig. 3), likely due to human interventions such as intensified
431 pumping during dry years, which disrupt the natural recharge-storage relations. In contrast, the DEM
432 showed a strong and consistent correlation, particularly at larger lags, reflecting the dominant role of
433 topography in controlling regional groundwater distribution and storage potential. Interestingly, the DEM-
434 groundwater level correlations persisted across all periods (see Fig. 3a, d, g, j). In contrast, cross-
435 covariances involving precipitation were more variable and short-ranged, indicating localized influence or
436 a stronger dependency on climatic anomalies. Spatial range estimates for groundwater level semi-
437 variograms varied from 435 to 812 km for periods 1 and 2. However, when disaggregated by
438 hydrogeological unit, much shorter ranges (73 km and 151 km for periods 3 and 4, respectively) were
439 observed in fractured aquifers, reflecting more localized variability. Porous aquifer systems, by contrast,
440 exhibited much longer correlation ranges (632 km and 491 km for periods 3 and 4, respectively), consistent
441 with their higher transmissivity.

442 Although period-specific variogram analyses indicate broadly stable spatial correlation structures,
443 differences in data density and spatial coverage among periods introduce uncertainty in the direct
444 comparison of variogram parameters. In particular, periods with fewer observations yield less robust
445 variogram estimates at larger spatial scales. This limitation is inherent to long-term groundwater datasets
446 compiled from heterogeneous monitoring networks and underscores the importance of interpreting
447 temporal changes in spatial structure cautiously.

448 The adopted variogram and cross-variogram modelling strategy prioritizes stability and comparability
449 across periods over detailed representation of local-scale heterogeneity. While alternative model forms or
450 anisotropic structures could locally improve interpolation performance, their influence at the continental
451 scale is expected to be secondary relative to data density, temporal aggregation, and network
452 configuration. This trade-off is well recognized in large-scale geostatistical applications, where sampling
453 design and scale effects often dominate uncertainty propagation (Gringarten and Deutsch, 2001; Lark,
454 2012).

455 The nugget-to-sill ratios across the data pairs provide further insight into data quality and spatial coherence.
456 For the DEM and groundwater levels, the nugget effect was minimal, suggesting high data reliability and
457 low measurement error. However, for the first period, the precipitation and groundwater cross-covariances
458 exhibited higher nugget-to-sill ratios, indicating weaker spatial coherence, likely due to both natural
459 variability and anthropogenic interference.

460 These fitted spatial relationships form the basis for the subsequent cokriging interpolation, enabling the
461 incorporation of secondary data with varying degrees of spatial dependence on the primary groundwater
462 level measurements.

463 ### 3.3. Spatial distribution of the groundwater level

464 Fig. 4 presents maps of the groundwater levels for periods 1 and 2 interpolated using (1) simple kriging
465 without secondary data, (2) cokriging using DEM, (3) cokriging using the average groundwater level of the
466 four periods, and (4) cokriging using precipitation as a secondary data. Groundwater level observations
467 were first aggregated by study period (1965–1984, 1985–1994, 1995–2004, 2005–2020) to calculate
468 period-average values at each observation point. These period-average values were then interpolated
469 spatially using kriging on a 4 km × 4 km grid to generate representative groundwater maps for each period.

The maps generated by simple kriging without secondary data show some variability in the eastern half of the region where data are available. However, in the data-sparse western regions, the interpolated groundwater level is close to the ensemble mean of the period. In contrast, when DEM was used as a secondary data source, the interpolated groundwater levels showed small-scale variability, with lower groundwater levels in low-lying areas and higher groundwater levels in elevated regions, particularly in the mountainous regions of northern Spain. Previous groundwater studies confirm the relationship between land surface elevation and groundwater levels and have shown that groundwater levels are often greater in higher elevation regions due to greater recharge conditions and lower evapotranspiration (Ruiz et al., 2023; Muhs, 2020; Somers and McKenzie, 2020).

The third interpolation scheme incorporates the time-averaged groundwater level over the entire period (1965-2020). The rationale for incorporating the average groundwater level data is the relatively low fluctuation of groundwater levels over time, which allows data acquired during different time spans to be used as a predictor of earlier (or future) conditions. This is supported by the high correlation between groundwater levels of the different periods and the time-average (Fig. 3). In areas without data, cokriging rescales the secondary data based on its correlation scattergram. Hence, including average groundwater levels helps reduce interpolation uncertainties, particularly in regions with no monitoring wells, resulting in more consistent interpolation maps with lower kriging variances.

Incorporating the precipitation variable in the fourth period had an insignificant impact on predicting groundwater levels. The maps generated showed minimal variations from those created without any secondary data. The irrelevance of precipitation, as a secondary variable, results from the low correlation observed between groundwater levels and annual precipitation (Fig. 3).

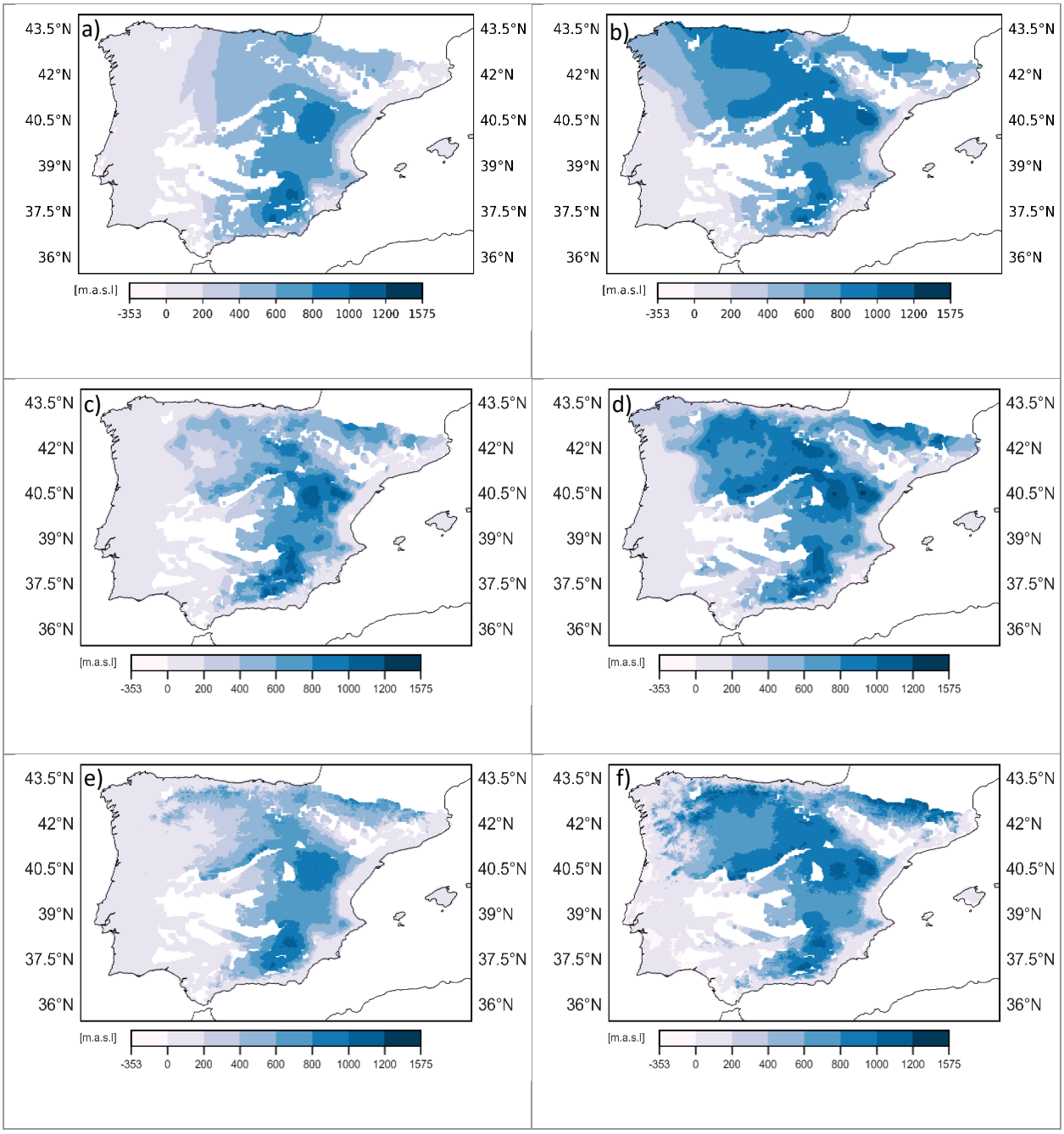
a)
b)
c)
d)
e)
f)
43.5°N
42°N
40.5°N
39°N
37.5°N
36°N
[m.a.s.l]
-353 0 200 400 600 800 1000 1200 1575

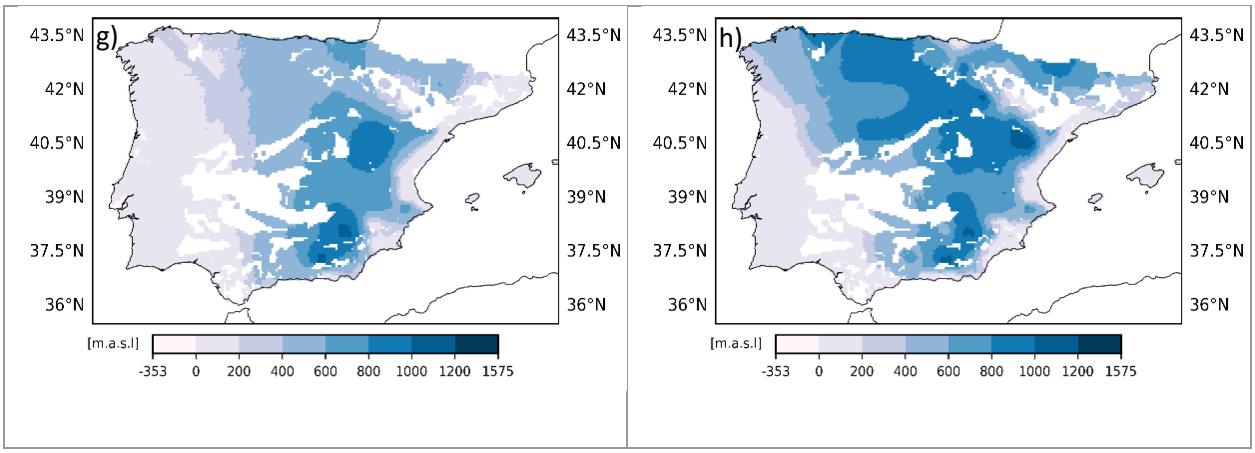

Fig. 4. Groundwater level maps for the Iberian Peninsula for period 1 (left column) and period 2 (right column); (a, b) without secondary data; (c, d) with average groundwater level as a secondary data; (e, f) with DEM as a secondary data; (g, h) with annual precipitation as a secondary data.

The estimated groundwater levels for the third and fourth periods generated using cokriging with the DEM data are presented in Figs. 5a, 5b. The estimated maps computed using simple kriging after segmenting the data into independent subgroups depending on the hydrogeological units they fall in (Fig. 3) are given in Figs. 5c, 5d.

The inclusion of the DEM as a secondary variable effectively reproduced the large-scale topographic patterns, especially in areas lacking observations of the groundwater levels. The map of groundwater levels obtained using the DEM for the fourth period showed more detailed spatial patterns than those presented in the third period, mainly due to higher data density. Higher groundwater levels were estimated in higher elevation areas, especially in mountainous regions where recharge of the groundwater system is more likely due to higher precipitation, lower groundwater extraction, and lower water losses through evapotranspiration. Conversely, lower groundwater levels were estimated in low-lying areas. This is consistent with the maps produced for periods 1 and 2 and with studies in Mediterranean climates, which indicate that topography plays a crucial role in the distribution of groundwater levels, mainly through the processes of recharge and subsurface water infiltration (e.g., Owuor et al., 2016; Somers and McKenzie, 2020).

509 The groundwater level map created by incorporating the hydrogeological units shows similar spatial
510 patterns of groundwater distribution, with only minor differences resulting from the underlying
511 hydrogeological factors. Groundwater levels in fractured and fissured aquifers were relatively high.
512 Conversely, relatively lower groundwater levels were estimated for less significant aquifers. Dividing the
513 data into subgroups based on the hydrogeological units is justified because certain hydrogeological units
514 are more suitable for groundwater storage and recharge and are, therefore, more likely to exhibit
515 groundwater level fluctuations, as noted in Manna et al. (2019). The inclusion of DEM data had a limited
516 impact on the estimation compared to using hydrogeological units.

517 Examination of Figs. 4 and 5 shows that groundwater level estimates for the third and fourth periods in the
518 western part of the Iberian Peninsula and the coastal areas are relatively lower than those of the first and
519 second periods. In addition, groundwater levels are relatively lower in the third and fourth periods in north-
520 eastern Spain (Catalonia), southern Spain (mainly in the Guadalquivir basin, Andalusia), eastern Spain
521 (Valencia and Catalonia) and in the central (Ribatejo and Oeste regions) and southern (Algarve aquifer)
522 parts of Portugal due to the relatively large number of irrigation wells in these regions (Carreira et al., 2014).
523 Examination of the interpolated maps (Figs. 5-6) shows that the spatial variability of the groundwater level
524 is much larger than the temporal variability. The groundwater levels vary from near zero in coastal areas to
525 as high as 1500 m in the central high elevation areas of the Peninsula. On the other hand, temporal
526 variability between periods varies locally, reflecting differences in hydrogeological conditions.

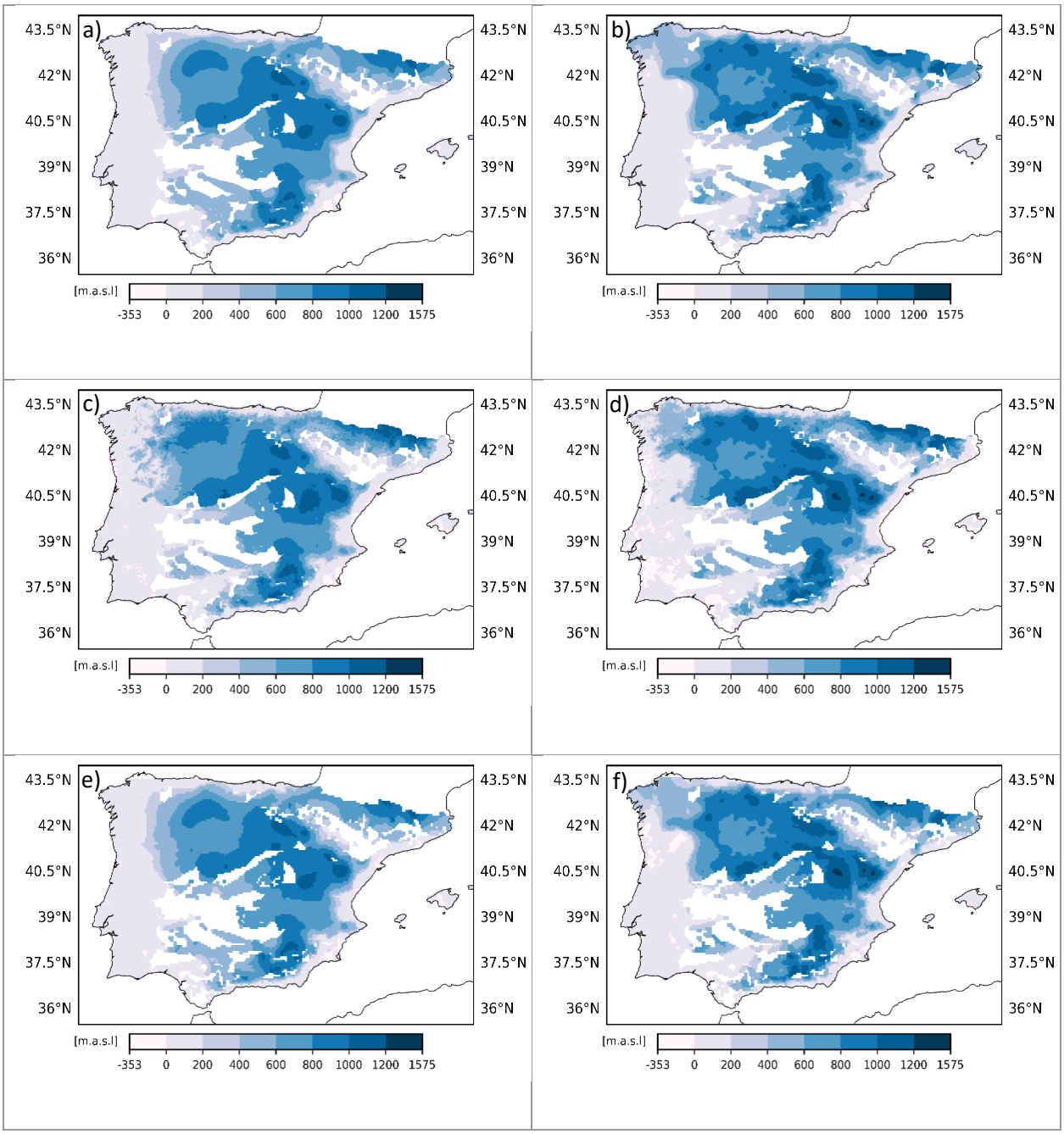

527 **Fig. 5.** Groundwater level maps for the Iberian Peninsula for periods 3 (left column) and 4 (right column).

528 (a, b) not using any secondary data, (c, d) using the DEM as a secondary data; (e, f) t segmenting the data

529 based on hydrogeological units.

530 ### 3.4. Validation of estimated groundwater level

Table 2 presents cross-validation of the predicted groundwater levels for the various schemes. Table 2 contains the RMSE and the ME for the different periods and interpolation schemes considered. Model performance was evaluated by leave-one-out cross-validation: water levels at each observation location were sequentially withheld, and the groundwater level at the observation location was predicted from the remaining data. The Root Mean Square Error (RMSE) and Mean Error (ME) were averaged across all withheld locations. In addition, kriging variance maps were also used to evaluate the different interpolation methods.

For the first and second periods, kriging using only the observed groundwater levels without considering additional secondary data resulted in high RMSE values, reflecting the scarcity of data. The inclusion of precipitation did not improve the error either. This is to be expected, as the correlation between the groundwater level and precipitation was low (Fig. 3).

Cokriging using the average groundwater level as a secondary variable has the smallest cross-validation RMSE, indicating improved interpolation of groundwater levels. However, the ME value is not the lowest (in absolute value), suggesting that although this interpolation scheme performs well in terms of error size, it introduces some bias. This bias is due to the likely decline in groundwater levels that the Iberian Peninsula has experienced in recent decades (Xanke and Liesch, 2022), which is not captured when the time-average groundwater is used in the interpolation.

The inclusion of the DEM for the first and second periods did not lead to lower RMSE and ME compared to using average groundwater levels as secondary data or with no secondary data. Two factors may have contributed to this result. The inclusion of the DEM in the kriging scheme also leads to a negative bias, which appears as a negative ME value. Moreover, groundwater head data are concentrated in the eastern part of the peninsula, with practically no data in the western part in these two periods. As such, while the DEM data may have contributed to the estimation of the groundwater levels in the western part, which

554 lacks data, this does not translate into a reduced RMSE and ME in cross-validation because the data
555 locations are concentrated in the eastern part of the study area.

556 **Table 2.** Cross-validation for groundwater level estimates for the four periods, using the different secondary
557 data.

Period	Secondary variable	RMSE (m)	ME (m)
First period (1965-1984)	-	105.060	- 6.065
	Average groundwater level	72.854	- 7.105
	DEM	88.560	- 17.603
	Precipitation	141.901	- 0.158
Second period (1985-1994)	-	75.101	- 3.100
	Average groundwater level	27.162	- 2.883
	DEM	61.556	- 23.758
	Precipitation	85.415	- 3.449
Third period (1995-2004)	DEM	67.018	- 12.874
	Hydrogeological units	69.78	- 1.72
Fourth period (2008-2020)	DEM	58.372	- 6.312
	Hydrogeological units	66.19	- 0.74

558 *RMSE: root mean square error (m), ME: mean error (m).

559 Including the hydrogeologic units as a "hydrogeology constraint" for the third and fourth periods does not
560 improve prediction accuracy compared to the DEM-based interpolation. Table 2 shows that kriging without
561 secondary data consistently yields the largest prediction errors across all periods, providing a clear baseline
562 against which the relative performance of the cokriging configurations can be evaluated. As shown in Table
563 2, the RMSE values are 69.78 m and 66.19 m, while the ME values are -1.72 m and -0.74 m, respectively,
564 slightly higher than those achieved with the DEM scheme. This suggests that incorporating hydrogeologic
565 units offers limited gain in predictive performance, with the benefit mostly concentrated in areas lacking
566 groundwater level observations.
567 Reported improvements in interpolation performance should therefore be interpreted as indicative of
568 relative model behavior rather than statistically significant differences. In large-scale groundwater
569 mapping, validation metrics primarily serve to identify consistent performance patterns across space, while
570 robustness and physical plausibility are prioritized over formal hypothesis testing. Similar interpretative

571 approaches have been adopted in other regional and continental groundwater assessments characterized
572 by spatial dependence and heterogeneous monitoring networks (de Graaf et al., 2020; Gleeson et al.,
573 2021b).
574 Maps of the kriging variance corresponding to the first and second periods for the different secondary
575 variables considered are shown in Fig. 6. Similar plots, not shown here, can be generated for the third and
576 fourth periods. The kriging variance represents uncertainty in the interpolated groundwater levels,
577 primarily driven by the density and distribution of observation points. It is lower in well-sampled areas and
578 higher where data are sparse, reflecting confidence in the interpolation rather than the natural variability
579 of groundwater levels. The uncertainty maps for the first and second periods, especially for models with
580 DEM and mean groundwater levels, show a general pattern of lower uncertainty in areas with higher data
581 density and more uniform terrain features. Regions with sparse data, particularly in the western part of the
582 Iberian Peninsula, and regions with complex terrain were associated with higher uncertainties. These maps
583 indicate areas of significant uncertainty where future monitoring wells can be potentially placed (Lorenzo-
584 Lacruz et al., 2017).

585 Overall, the cokriging technique incorporating average groundwater level as a secondary variable in periods
586 1 and 2 or those including hydrogeologic information (periods 3 and 4) resulted in the most accurate and
587 spatially consistent patterns of groundwater levels across the Iberian Peninsula and a significant
588 improvement in prediction compared to other interpolation schemes.

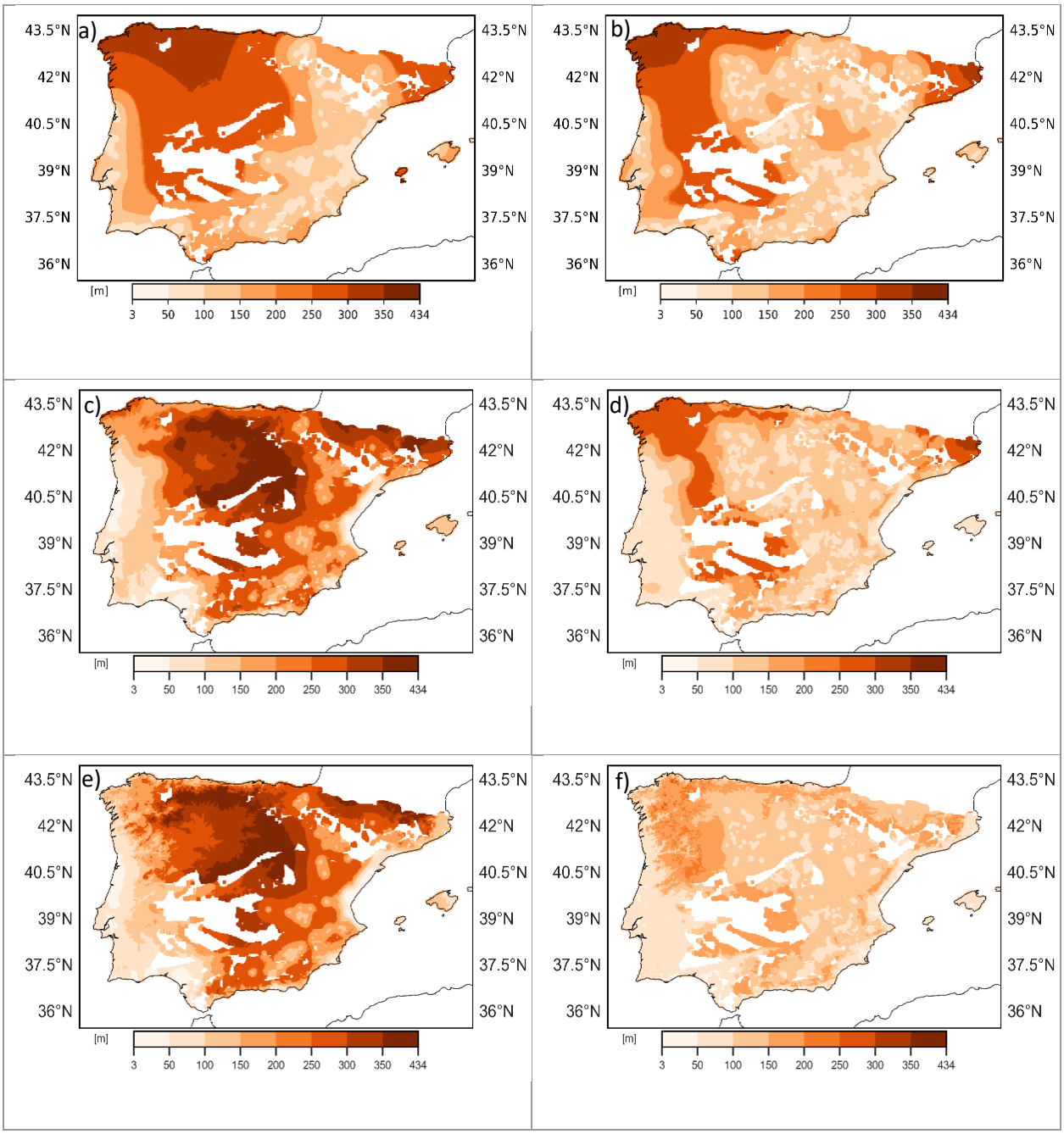
a)
b)
c)
d)
e)
f)
43.5°N
42°N
40.5°N
39°N
37.5°N
36°N
[m]
3 50 100 150 200 250 300 350 434

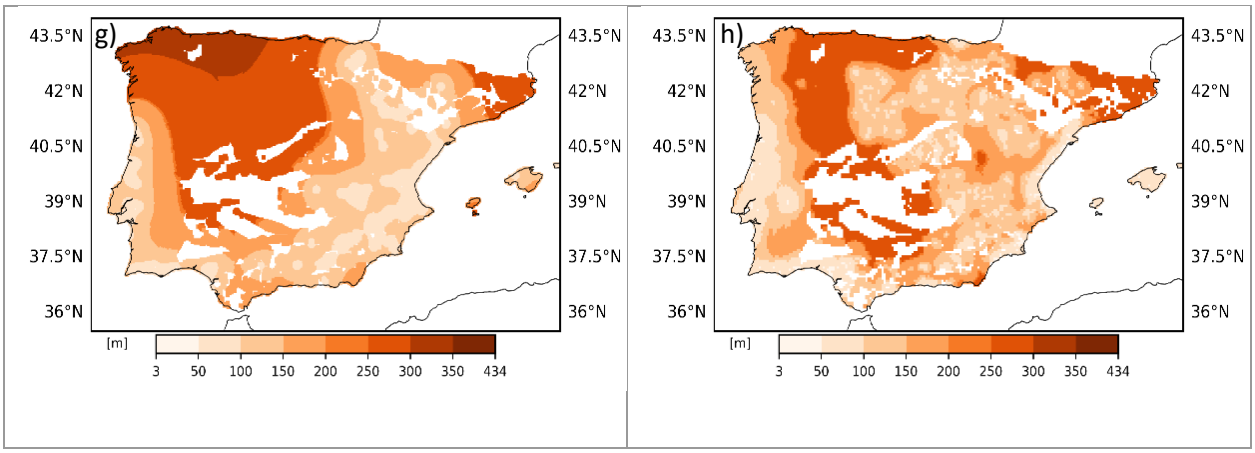

589 **Fig. 6.** Maps of the groundwater level kriging variance for the first period (Left column) and the second
590 period (Right column). (a, b) No secondary data; (c, d) average groundwater level; (e, f) DEM; (g, h) annual
591 precipitation as a secondary variable.

592 ## 4. Discussion

593 This study highlights two key challenges in the interpolation of hydrological data: (i) the availability of in-
594 situ data varies significantly in space and time, with past periods often characterized by data scarcity; (ii)
595 while kriging-based techniques are widely used at the local scale, the robustness when applied to a large
596 area characterized by complex hydrogeology is much less frequently examined. To examine these two
597 issues, we focus in this study on the estimation of groundwater levels over the entire Iberian Peninsula
598 using a unique dataset consisting of groundwater level measurements from 3882 wells spanning 50 years.
599 The intended use of the interpolated groundwater level is to support regional-to-national-scale
600 assessments of groundwater patterns and their relation to landscape characteristics and long-term
601 environmental conditions. It provides a baseline for understanding broad-scale groundwater variability and
602 for evaluating the added value of secondary datasets. Interpolated data are not intended for site-specific
603 management or detailed aquifer modelling, due to their spatial resolution and the use of decadal averages.
604 The interpolated maps should not be interpreted as showing continuous aquifer systems across the Iberian
605 Peninsula. Lithological heterogeneity, impermeable boundaries, and aquifer discontinuities locally control

606 groundwater dynamics. The maps represent spatially generalized patterns useful for regional assessment,
607 rather than depicting hydraulic connectivity at the local scale.
608 At the Iberian scale, spatial variability in groundwater levels is much larger than temporal variability. In this
609 study, temporal patterns were evaluated through comparisons of interpolated maps, but this approach
610 may obscure small but relevant temporal changes. Alternative approaches, such as first producing a
611 baseline spatial interpolation and then mapping differences between periods, or interpolating the depth to
612 groundwater below the land surface, could enhance the detection of temporal signals. To overcome the
613 data scarcity of past periods, we explore the benefits of including secondary data in the interpolation
614 processes.
615 A key strength of this study is the integration of a large, multi-period groundwater dataset spanning more
616 than five decades, enabling spatially consistent regional-scale comparison across the Iberian Peninsula.
617 However, the spatial and temporal heterogeneity of the monitoring network remains a primary limitation.
618 Regions with dense well coverage yield well-constrained groundwater level patterns, whereas smoother
619 interpolated surfaces occur in data-sparse areas. This contrast reflects the balance between observational
620 control and reliance on spatial covariance structures inherent to large-scale geostatistical groundwater
621 mapping (Fan et al., 2019; Ruybal et al., 2022).
622 The assumption of spatial continuity is appropriate at the regional scale of this study, where the objective
623 is to identify large-scale groundwater level patterns rather than resolve local hydrogeological complexity.
624 Nevertheless, the absence of detailed hydrogeological parameters, groundwater abstraction records, and
625 well-construction metadata limits the attribution of groundwater levels to specific aquifer units or pumping
626 stresses. In multi-layered aquifer systems, the lack of information on screened intervals prevents
627 differentiation between shallow and deep groundwater responses, a common constraint in regional
628 groundwater assessments (Gleeson et al., 2020; de Graaf et al., 2019).

Due to the limited availability of groundwater level observations in certain areas, particularly in the west of the Iberian Peninsula in past decades, the estimation of groundwater levels in these areas based solely on observed head levels is associated with a high level of uncertainty. Similar conditions are encountered in numerous other locations, particularly in earlier times when monitoring data were scarce. To overcome this limitation, readily available secondary data can indirectly capture the spatial variations in groundwater levels, provided they show a clear correlation to the groundwater level. An added challenge when secondary data are considered at the regional scale is the representative scale of the different data. While groundwater level data are point measurements, the support volume of secondary data can be significantly different. The time resolution of the different data is another issue that can influence the correlation between the different parameters and the contribution to the interpolation.

In this analysis, three secondary variables were considered using cokriging for the estimation of the groundwater level across the Iberian Peninsula: DEM, precipitation, and observer groundwater level data at later times. In addition, the groundwater level map was also estimated using kriging by dividing the data into subsets depending on the hydrogeologic units in which the data fall.

In this study, groundwater levels were evaluated against individual secondary datasets (precipitation, DEM, and average groundwater level). This allowed us to determine which secondary variable contributed the most relevant information for predicting groundwater levels. Nonetheless, we acknowledge that such a design cannot capture potential interactions among secondary variables. More comprehensive approaches, such as the multi-dataset integration applied by Koch et al. (2019), offer a promising way forward. Future research can extend our framework by combining multiple secondary datasets in joint analyses to better represent the complexity of large-scale groundwater systems. Compared with multi-dataset studies such as Koch et al. (2019), our analysis included fewer secondary datasets. This choice was constrained by data availability across the Iberian Peninsula and the need for spatial consistency.

652 The results show that DEM has a significant influence on the distribution of the groundwater level. This
653 high correlation (R^2 = 0.98) was observed across the Iberian Peninsula and through the four periods
654 spanning more than 50 years. The observed positive correlation between land surface elevation and
655 groundwater levels persists across all periods. This suggests that variations in groundwater levels driven by
656 climatic or extraction pressures do not substantially weaken the observed correlation, consistent with
657 Mediterranean studies showing that groundwater–topography relationships remain largely stable under
658 varying hydroclimatic conditions (Custodio et al., 2016). Terrain features affect groundwater recharge by
659 influencing surface water flow, infiltration, and groundwater storage capacity. Although higher-elevation
660 areas can provide additional storage in fractured or karstic aquifers, groundwater abstraction is more
661 commonly concentrated in valleys and lowlands, where the water table lies closer to the surface, and
662 aquifers are more accessible. As such, in regions lacking the groundwater level observations, the high
663 correlation between the groundwater level and the DEM allows for the enhanced interpolation of
664 groundwater levels that would otherwise not be possible. The inclusion of the DEM as a secondary variable
665 is supported by earlier findings that groundwater tables tend to form a subdued replica of surface
666 topography (Haitjema and Mitchell-Bruker, 2005).

667 The correlation between the groundwater levels at a certain point in time and the long-term average
668 groundwater levels is evident from the scatterplots. Groundwater systems in regions such as the Iberian
669 Peninsula exhibit seasonal fluctuations and gradual recharge (Moutahir et al., 2017). The stability of
670 groundwater in the study area over time means that, in the absence of in-situ groundwater levels, its long-
671 term average can be a useful surrogate, leading to improved mapping of the groundwater levels.

672 Somewhat counterintuitively, precipitation showed a limited correlation with groundwater levels. It is
673 generally recognized that precipitation significantly influences groundwater levels, especially in
674 Mediterranean regions where precipitation can be heavy in some seasons but erratic. The significant

change in precipitation patterns in the Iberian Peninsula over time and space may have contributed to this weak correlation. In the Iberian Peninsula, precipitation patterns exhibit complex spatial patterns with highly variable intensities and interference by surface cover. These factors contribute to the complexity of the recharge process; hence, the response of groundwater systems to precipitation is strongly attenuated as a result of factors such as insufficient rainfall, low soil infiltration rates resulting in a large lag between recharge and fluctuations in the water table (Lorenzo-Lacruz et al., 2017). The thickness of the unsaturated zone is also an important factor, as a deep unsaturated zone can significantly delay recharge transmission to the aquifer and thus reduce the immediate responsiveness of groundwater levels to precipitation. In addition, anthropogenic activities such as groundwater abstraction, irrigation, and land use change affect groundwater levels and potentially mask the direct effects of annual precipitation.

The weak correlation shown in this study suggests that annual precipitation alone cannot explain groundwater fluctuations. Examination of previous studies conducted in the Iberian Peninsula has come to results that support this conclusion, showing that groundwater recharge is often influenced by multiple factors, such as soil properties, subsurface flow, and aquifer permeability, rather than precipitation alone (Hartmann et al., 2017; Lorenzo-Lacruz et al., 2017).

A key property of cokriging is its reliance on the strength and spatial consistency of the correlation between the primary variable and auxiliary datasets. When this relationship is weak or spatially variable, secondary variables receive low weights, and cokriging predictions approach those of simple kriging (Wackernagel, 2013; Journel and Huijbregts, 2016). Under such conditions, gains in accuracy are limited, and prediction uncertainty remains relatively high. In this study, this behavior is observed in regions where secondary variables exert only a weak control on groundwater levels (such as the precipitation secondary parameter), resulting in modest improvements over the baseline. Similar conclusions have been reported in the

literature, underscoring that cokriging is most effective when auxiliary data represent dominant physical controls rather than weak statistical associations (Kumar et al., 2021; Li et al., 2023).

It is important to clarify that correlations between groundwater levels and secondary datasets (precipitation, DEM, and average groundwater level) represent statistical associations rather than methodological improvements. While these associations help identify relevant large-scale controls, they should not be interpreted as direct enhancements of interpolation accuracy. The kriging variance maps highlight that interpolation uncertainty was greatest during the earliest period (1965–1984), primarily reflecting the limited spatial coverage of groundwater observations. In subsequent periods, uncertainty progressively decreased with the expansion of the monitoring network, while the use of average head as a secondary variable further minimized estimation variance due to its strong spatial correlation with groundwater levels. Uncertainty was partly addressed in this study through cross-validation metrics and co-kriging variance maps, which provide a measure of interpolation error. Nevertheless, these do not fully account for the robustness of temporal differences, and uncertainties may still influence the interpretation of changes between periods.

Compared to simple kriging, cokriging with secondary variables yields lower prediction errors and more spatially coherent groundwater level patterns, particularly in sparsely monitored regions. Cokriging also reduces and spatially constrains prediction uncertainty where auxiliary variables provide complementary information, consistent with findings from other regional groundwater mapping studies (Brunner et al., 2021; Ruybal et al., 2022).

The consistently low cross-validation errors obtained across periods indicate that the interpolated groundwater patterns are not artifacts of temporal data reuse, but rather reflect stable spatial relationships supported by the available observations. Although formal sensitivity analyses based on alternative cokriging

719 formulations can provide additional insight, their implementation at a continental scale is often constrained
720 by uneven data density and computational cost (Reinecke et al., 2020; Gleeson et al., 2021a).

721 Future studies should apply more comprehensive geostatistical approaches (e.g., conditional simulation)
722 to better quantify uncertainties when comparing temporal patterns.

723 Temporal non-stationarity also affects the interpretation of cokriging results. The statistical relationships
724 between groundwater levels and secondary variables such as precipitation or elevation may evolve due to
725 changes in recharge regimes, groundwater abstraction, or land-use patterns (Fan et al., 2013). By
726 performing cokriging separately for each period and relying on temporally averaged groundwater
727 conditions, the present analysis prioritizes identifying persistent, large-scale spatial patterns over transient
728 or short-term dynamics. As a result, cokriging relationships should be interpreted as period-specific
729 representations of prevailing conditions, and comparisons across periods should focus on broad regional
730 contrasts rather than localized temporal changes. This interpretation is consistent with continental-scale
731 groundwater studies emphasizing scale-dependent inference (Döll et al., 2014).

732 Although unit-specific interpolation respects hydrogeological boundaries, it may result in edge effects or
733 discontinuities at unit boundaries. No attempt was made to smooth out these discontinuities. The use of
734 hydrogeological units, although not explicitly included as a secondary variable in the interpolation scheme,
735 facilitated the categorization of groundwater levels based on the different hydrogeological properties of
736 the various aquifers. The distinction between fractured, fissured, porous, and minor aquifers provides a
737 valuable context to understand the spatial patterns of projected groundwater levels. Previous studies show
738 that aquifer properties, such as permeability and porosity, strongly influence groundwater systems, playing
739 a crucial role in determining groundwater flow and groundwater abstraction (Hartmann et al., 2017; Rao
740 et al., 2022). The hydrogeological data from this study helped to identify regions where groundwater levels
741 are influenced by geological factors rather than topographic features alone. By performing the

742 interpolation for each hydrogeological unit separately, local means and variograms within each
743 hydrogeological unit are defined and utilized in the interpolation scheme, leading to reduced error
744 statistics.

745 In summary, the results of this study emphasize the advantages of combining secondary data, such as
746 topographic and hydrogeological characteristics, in predicting groundwater levels. The cokriging method is
747 demonstrated to be an effective interpolation tool for identifying large-scale spatial groundwater level
748 patterns. The inclusion of additional secondary data and hydrogeological information in the interpolation
749 scheme could further improve the accuracy and reliability of groundwater level estimation in the Iberian
750 Peninsula and comparable Mediterranean regions.

751 Global-scale groundwater models, such as transient two-layer simulations from (de Graaf et al., 2017) and
752 the steady-state groundwater levels presented by Ben-Salem et al. (2023), provide mechanistic
753 representations of groundwater dynamics over extensive spatial and temporal scales. While the transient
754 models integrate hydrological processes and assumptions regarding recharge, aquifer transmissivity, and
755 boundary conditions, our interpolated groundwater heads are based solely on observed measurements
756 and reflect the empirically constrained state of the system. Consequently, these observational datasets
757 complement large-scale models by providing an independent benchmark for model evaluation and
758 calibration, enabling a more robust assessment of regional groundwater dynamics while acknowledging
759 methodological differences and resolution constraints. Groundwater heads are mainly determined by
760 aquifer geometry, boundary conditions, and drainage surfaces. Precipitation was used here as a secondary
761 dataset to indicate regional hydroclimatic patterns, but absolute water table elevations are ultimately
762 governed by net recharge, which integrates precipitation, evapotranspiration, and lateral flow.

763 The secondary datasets used in this study are useful in capturing large-scale hydroclimatic and
764 physiographic patterns that influence groundwater levels. However, their role is best understood as

765 providing regional context rather than direct controls on local groundwater conditions, which are
766 influenced by complex spatial and temporal natural processes (such as precipitation, evaporation, aquifer
767 boundaries) and anthropogenic factors (such as agriculture, extraction, and land use) that are difficult to
768 define, especially over large areas. The datasets used in the study help to improve the interpretability of
769 interpolated groundwater heads, while acknowledging that unresolved local-scale variability remains.
770 At the regional scale, spatially consistent groundwater level maps provide a robust basis for strategic
771 groundwater management, supporting the identification of depletion-prone areas, recharge-dominated
772 zones, and priorities for monitoring network optimization. While the results are not intended for site-
773 specific abstraction decisions, they are well-suited for basin-scale assessments, inter-regional comparisons,
774 and transboundary water governance, where internally consistent spatial information is required. More
775 generally, this study demonstrates how long-term groundwater observations can be systematically used
776 through temporal aggregation to derive stable large-scale patterns despite evolving monitoring networks.
777 The results also highlight the importance of selecting secondary variables that are physically meaningful,
778 spatially continuous, and temporally consistent, such as topography and long-term precipitation, thereby
779 enhancing the transferability of the approach to other regions characterized by sparse or heterogeneous
780 groundwater data availability (Wada et al., 2010; Gleeson et al., 2020).
781 The results of this analysis highlight the inherent variability of groundwater levels in the Iberian Peninsula
782 due to natural and anthropogenic processes. Various factors, such as topography, geological heterogeneity,
783 climate variability, and land use changes, contribute to the fluctuations in groundwater levels. Establishing
784 a fundamental understanding of historical groundwater variability serves as a reference point for assessing
785 the impact of future natural variability and human activities on groundwater resources. Further research
786 could focus on characterizing and analyzing specific drivers responsible for groundwater level fluctuations,
787 including the effects of climate change, groundwater recharge processes, and land use change.

In addition, the analysis presented here can identify depleted groundwater systems that have undergone severe temporal changes and would therefore require more attention and conservation efforts against further overexploitation. The drop is most notable in areas with intensive groundwater use, suggesting that abstraction is a key driver of the observed trend. This supports the rationale for a temporal segmentation approach to better capture evolving regional groundwater dynamics.

Another important benefit of this study is the identification of areas where groundwater resources are under significant pressure. In particular, the regions in the southeast and south of the Iberian Peninsula, including the Guadalquivir and Segura River basins, show considerable groundwater depletion. These areas, as well as parts of the eastern coastal areas, face major challenges due to a combination of long periods of drought, excessive groundwater abstraction, and high agricultural demand. Identifying these regions as critical zones for groundwater stress will help prioritize targeted management and conservation strategies. Thus, appropriate strategies would be needed to mitigate these impacts. These include, for example, growing drought-tolerant crops that require little water, crop rotation, and using smart farming practices to increase efficiency and reduce environmental impact.

The spatial groundwater level patterns identified in this study are broadly consistent with recent regional and basin-scale investigations across the Iberian Peninsula, which highlight the combined influence of hydro-climatic variability, aquifer characteristics, and monitoring network configuration on groundwater dynamics. Recent assessments have reported long-term declines in groundwater levels in several Iberian aquifers, particularly in semi-arid regions, driven by reduced recharge and increased abstraction pressures (Ferreira Branco et al., 2024; Rouhani et al., 2025). Regional assessments for major basins such as the Guadiana, Segura, and Ebro document persistent groundwater level declines, often on the order of decimeters to over one meter per year depending on local conditions (Custodio et al., 2016; Llamas and Martínez-Santos, 2005). The regional patterns obtained in this study reflect similar large-scale gradients, supporting the robustness of the period-based approach adopted here.

A major strength of this work lies in the compilation and harmonization of a large, multi-decadal groundwater dataset spanning more than five decades, enabling comparison of groundwater level distributions across distinct periods. Nevertheless, the spatially irregular distribution of monitoring stations represents a key limitation. Areas with high monitoring well density exhibit more detailed and better-constrained interpolation of groundwater surfaces with lower kriging variances (Fig. 6), whereas smoother spatial patterns are obtained in regions with sparse data coverage. Some reduction in the variance map was obtained when the secondary data were incorporated in the cokriging procedure, with the variance reduction dependent on the correlation of the secondary variable with the groundwater level. This behaviour is consistent with similar geostatistical and large-scale groundwater modelling studies, which demonstrate that interpolation accuracy and uncertainty are strongly dependent on observation density and spatial configuration (e.g., Giese et al., 2025). Consequently, while the produced maps are suitable for identifying broad regional trends, caution is required when interpreting the interpolated maps in data-scarce areas, which would necessitate the incorporation of finer-scale features information.

This study is subject to several limitations that are intrinsic to large-scale groundwater assessments and should be considered when interpreting the results. First, the spatial resolution of the interpolated groundwater surfaces represents a compromise between regional coverage and data availability, meaning that local-scale heterogeneity, vertical hydraulic gradients, and well-specific conditions cannot be resolved. Second, uncertainty increases in areas with sparse or unevenly distributed monitoring networks, where groundwater level estimates are more strongly influenced by secondary variables than by direct observations. Third, the temporal aggregation of measurements within multi-year periods reduces short-term variability and non-stationarity but may obscure localized responses to groundwater abstraction or land-use change. These scale effects and sources of uncertainty are well recognized in continental-scale groundwater studies and underscore the importance of interpreting interpolated groundwater levels as regional indicators rather than precise local representations (Fan et al., 2019; Cuthbert et al., 2019).

836 Accordingly, the results are intended to support regional-scale assessments and comparative analyses
837 rather than site-specific groundwater management decisions. Future work should focus on extending the
838 current spatial framework to support uncertainty-aware analyses of groundwater level trends and their
839 climatic and anthropogenic drivers, with improved data harmonization and complementary hydro-climatic
840 information.

841 ## 5. Conclusions

842 This study investigated the usefulness of various secondary data using kriging-based interpolation schemes
843 applied on a large scale, namely the Iberian Peninsula. The application of the proposed kriging-based
844 interpolation schemes was characterized by limited data availability, especially in the first and second
845 periods, in a complex geology. Relying solely on direct groundwater level observations led to the generation
846 of groundwater maps with a high degree of uncertainty. The integration of secondary data, specifically, the
847 DEM and groundwater observations from other periods, into the cokriging scheme, as well as hydrogeology
848 information, led to reduced uncertainty in the interpolation of the groundwater levels, allowing for
849 enhanced understanding of the variation of groundwater levels in the Iberian Peninsula. Although the
850 regional interpolation provides a coherent overview, the findings must be interpreted with caution, given
851 the pronounced geological heterogeneity and the discontinuous nature of aquifer systems across the
852 Iberian Peninsula. The results reveal broad spatial patterns but do not imply the presence of continuous
853 aquifer systems within such a geologically complex region.

854 The results of this study show that cokriging can be successfully applied to larger geographical areas with
855 complex hydrogeology, land use, and anthropogenic factors, pointing to the robustness of these
856 interpolation methods. By combining geostatistical techniques with readily available data, such as those
857 retrieved from earth observations that offer immense spatial coverage, improved mapping of hydrological
858 attributes can be achieved. Overall, this research contributes to the broader field of subsurface hydrology
859 by improving our understanding of long-term groundwater dynamics and demonstrating the effectiveness

of kriging-based schemes in such analyses, highlighting their implications for sustainable water resources management.

The proposed framework is transferable to regions with heterogeneous and temporally evolving groundwater monitoring networks, provided that analyses are conducted at appropriate spatial scales, temporal segmentation is used to limit non-stationarity, and secondary variables are selected for their physical relevance and spatial continuity. The study thus offers a practical template for using later-period observations in earlier decadal assessments and for improving spatial coherence in data-scarce settings through hydro-climatic covariates. Comparable approaches applied in large aquifer systems worldwide highlight the broader applicability of geostatistical methods for regional groundwater assessment beyond well-instrumented areas (Taylor et al., 2022; Bierkens et al., 2024).

Beyond the spatial analysis presented in this study, several avenues for future research emerge, particularly those aimed at relaxing some of the simplifying assumptions adopted here. A natural extension of this work is the investigation of the temporal evolution of groundwater levels through trend analysis, change-point detection, and attribution to climatic variability and anthropogenic pressures. Recent large-scale studies have demonstrated that groundwater responses to droughts and long-term climate variability are highly heterogeneous, reflecting differences in recharge processes, aquifer properties, and groundwater use (Ebeling et al., 2025; Giese et al., 2025; Rusli et al., 2024). However, robust temporal analyses require long, consistent, and well-documented monitoring records. In the Iberian Peninsula, such analyses are challenged by non-stationary observation networks, changes in station locations, variable measurement frequency, and evolving monitoring methodologies over the 1965–2020 period. Addressing these issues will require careful homogenization of time series, explicit treatment of data gaps and uncertainties, and, where possible, integration of auxiliary information on groundwater abstraction and land-use change. Future efforts that combine improved monitoring continuity with advanced statistical and hydrogeological frameworks will be essential for disentangling long-term groundwater trends from short-term variability.

884 Accordingly, the results of this study are intended to support regional-scale assessments, comparative
885 analyses across time periods, and strategic groundwater management discussions, rather than site-specific
886 or operational decision-making. While the adopted framework provides a consistent and reproducible
887 representation of large-scale groundwater level patterns, its applicability at finer spatial scales is
888 constrained by monitoring density, hydrogeological complexity, and temporal data aggregation.
889 Recognizing these scale-dependent limitations is essential to ensure appropriate use of large-scale
890 groundwater mapping products, as emphasized in recent continental and global groundwater assessments
891 (de Graaf et al., 2019; Bierkens et al., 2024).
892

References

Ahmadi, S. H., Sedghamiz, A., 2007. Geostatistical analysis of spatial and temporal variations of groundwater level. Environ Monit Assess. 129(1), 277-294. https://doi.org/10.1007/s10661-006-9361-z

Ahmed, S. and de Marsily, G., 1987. Comparison of geostatistical methods for estimating transmissivity using data on transmissivity and specific capacity. Water Resour. Res. 23, 1717-1737. https://doi.org/10.1029/WR023i009p01717

Allard, D., Chilès, J.-P., Delfiner, P., 2013. Geostatistics: Modeling spatial uncertainty. Math Geosci. 45, 377–380. https://doi.org/10.1007/s11004-012-9429-y

Asante, D., Appiah-Adjei, E. K., Asare, A., 2022. Delineation of groundwater potential zones using cokriging and weighted overlay techniques in the Assin Municipalities of Ghana. Sustain. Water Resour. Manag. 8(2), 55. https://doi.org/10.1007/s40899-022-00639-8

Bierkens, M.F.P., Wada, Y., 2023. Non-stationarity of groundwater systems under global change. Nat. Rev. Earth Environ. https://doi.org/10.1038/s43017-023-00421-7

Bierkens, M.F.P., Wada, Y., Döll, P., 2024. Global groundwater modeling and management. Nat. Rev. Earth Environ. https://doi.org/10.1038/s43017-024-00458-1

Ben-Salem, N., Reinecke, R., Copty, N. K., Gómez-Hernández, J. J., Varouchakis, E. A., Karatzas, G. P., Rode, M., Jomaa, S., 2023. Mapping steady-state groundwater levels in the Mediterranean region: The Iberian Peninsula as a benchmark. J. Hydrol. 626, 130207. https://doi.org/10.1016/j.jhydrol.2023.130207

Branco, M.F., Barbosa, S.V., Matos, J.X., 2024. Trend detection and depletion effects in groundwater-level time series of the Tagus–Sado Basin (Portugal). Sustain. Water Resour. Manag. https://doi.org/10.1007/s40899-024-01083-6

Brunner, P., Simmons, C.T., Cook, P.G., Therrien, R., 2021. Groundwater modeling at regional scale. Hydrogeol. J. https://doi.org/10.1007/s10040-021-02323-8

Brus, D.J., Heuvelink, G.B.M., Walvoort, D.J.J., 2011. Validation of spatial prediction models: theory and practice. Int. J. Geogr. Inf. Sci. https://doi.org/10.1080/13658816.2011.554673

Cardoso, R.M., Soares. PMM., Miranda, PMA., Belo-Pereira, M., 2013. WRF high-resolution simulation of Iberian mean and extreme precipitation climate. Int. J. Climatol. 33: 2591-2608. https://doi.org/10.1002/joc.3616

Carreira, P. M., Marques, J. M., Nunes, D., 2014. Source of groundwater salinity in coastline aquifers based on environmental isotopes (Portugal): Natural vs. human interference. A review and reinterpretation. Appl. Geochem. 41, 163-175. https://doi.org/https://doi.org/10.1016/j.apgeochem.2013.12.012

Cay, T., Uyan, M., 2009. Spatial and temporal groundwater level variation geostatistical modeling in the city of Konya, Turkey. Water Environ. Res. 81(12), 2460-2470. https://doi.org/10.2175/106143009x442961

Chávez García Silva, R., Borchardt, D., Reinecke, R., Copty, N.K., Barry, D.A., Heggy, E., Labat, D., Roggero, P.P., Rode, M., Gómez-Hernández, J.J., Jomaa, S., 2024. Multi-decadal groundwater observations reveal surprisingly

stable levels in southwestern Europe. Commun. Earth Environ. 5, 387. https://doi.org/10.1038/s43247-024-01554-w

Chilès, J.-P., Delfiner, P., 2012. Geostatistics: Modeling Spatial Uncertainty. Wiley.

Cuthbert, M.O., Gleeson, T., Moosdorf, N., Befus, K.M., Schneider, A., Hartmann, J., Lehner, B., 2019. Global patterns and dynamics of climate–groundwater interactions. Nat. Clim. Change 9, 137–141. https://doi.org/10.1038/s41558-018-0386-4

Custodio, E., 2002. Aquifer overexploitation: what does it mean? Hydrogeol. J. 10(2), 254-277. https://doi.org/10.1007/s10040-002-0188-6

Custodio, E., Cabrera, M. d. C., Poncela, R., Puga, L.-O., Skupien, E., del Villar, A., 2016. Groundwater intensive exploitation and mining in Gran Canaria and Tenerife, Canary Islands, Spain: Hydrogeological, environmental, economic and social aspects. Sci. Total Environ. 557-558, 425-437. https://doi.org/https://doi.org/10.1016/j.scitotenv.2016.03.038

Dahlke, H.E., Brown, A.G., Orloff, S., Putnam, D.H., O'Geen, T., 2018. Managed winter flooding of alfalfa recharges groundwater with minimal crop damage. Calif. Agric. 72. https://doi.org/10.3733/ca.2018a0001

de Graaf, I. E. M., van Beek, R. L. P. H., Gleeson, T., Moosdorf, N., Schmitz, O., Sutanudjaja, E. H., Bierkens, M. F. P., 2017. A global-scale two-layer transient groundwater model: Development and application to groundwater depletion. Adv. Water Resour. 102, 53-67. https://doi.org/https://doi.org/10.1016/j.advwatres.2017.01.011

de Graaf, I.E.M., Gleeson, T., van Beek, L.P.H. (Rens), Sutanudjaja, E.H., Bierkens, M.F.P., 2019. Environmental flow limits to global groundwater pumping. Nature 574, 90–94. https://doi.org/10.1038/s41586-019-1594-4

de Graaf, I.E.M., Gleeson, T., Sutanudjaja, E.H., van Beek, L.P.H., Bierkens, M.F.P., and Wada, Y., 2020. Large-scale assessment of groundwater depletion. Hydrol. Earth Syst. Sci. 24, 2667–2687. https://doi.org/10.5194/hess-24-2667-2020

de Marsily, G., 2021. Will we soon run out of water? Ann Nutr Metab. 76, 10-16. https://doi: 10.1159/000515019

Diodato, N., Seim, A., Ljungqvist, F. C., Bellocchi, G., 2024. A millennium-long perspective on recent groundwater changes in the Iberian Peninsula. Commun. Earth Environ. 5(1), 257. https://doi.org/10.1038/s43247-024-01396-6

Döll, P., Müller-Schmied, H., Schuh, C., Portmann, F.T., Eicker, A., 2014. Global-scale assessment of groundwater depletion and related groundwater abstractions: combining hydrological modeling with information from well observations and GRACE satellites. Water Resour. Res. 50, 5698–5720. https://doi.org/10.1002/2014WR015595

Dowd, P.A., Pardo-Igúzquiza, E., 2024. The many forms of co-kriging: A diversity of multivariate spatial estimators. Math. Geosci. 56, 387–413. https://doi.org/10.1007/s11004-023-10104-7

Ebeling, P., Musolff, A., Kumar, R., Hartmann, A., Fleckenstein, J.H., 2025. Groundwater head responses to droughts across Germany. Hydrol. Earth Syst. Sci. https://doi.org/10.5194/hess-29-2925-2025

ESRI, 2023. ArcGIS Pro 3.1. Environmental Systems Research Institute (ESRI), Redlands, CA, USA.

962 Erostate, M., Huneau, F., Garel, E., Ghiotti, S., Vystavna, Y., Garrido, M., Pasqualini, V., 2020. Groundwater-dependent
963 ecosystems in coastal Mediterranean regions: Characterization, challenges, and management for their
964 protection. Water Res. 172, 115461. https://doi.org/https://doi.org/10.1016/j.watres.2019.115461
965 Famiglietti, J.S., 2014. The global groundwater crisis. Nat. Clim. Change. 4, 945-948.
966 https://doi.org/10.1038/nclimate2425
967 Fan, Y., Li, H., Miguez-Macho, G., 2013. Global patterns of groundwater table depth. Science 339, 940–943.
968 https://doi.org/10.1126/science.1229881
969 Fan, Y., Li, H., Miguez-Macho, G., 2019. Global groundwater table depth. Science
970 https://doi.org/10.1126/science.aav4574
971 Font Tullot, I., 2000. Climatología de España y Portugal. Salamanca: Universidad de Salamanca, 422 pp.
972 Garrido, A., Martínez-Santos, P., Llamas, M. R., 2006. Groundwater irrigation and its implications for water policy in
973 semiarid countries: the Spanish experience. Hydrogeol. J. 14(3), 340-349. https://doi.org/10.1007/s10040-
974 005-0006-z
975 Gelati, E., Zajac, Z., Ceglar, A., Bassu, S., Bisselink, B., Adamovic, M., Bernhard, J., Malagó, A., Pastori, M., Bouraoui, F.,
976 de Roo, A., 2020. Assessing groundwater irrigation sustainability in the Euro-Mediterranean region with an
977 integrated agro-hydrologic model, Adv. Sci. Res., 17, 227–253, https://doi.org/10.5194/asr-17-227-2020
978 Giese, M., Caballero, Y., Hartmann, A., Charlier, J.-B., 2025. Trends in long-term hydrological data from European karst
979 areas: insights for groundwater recharge evaluation. Hydrol. Earth Syst. Sci. https://doi.org/10.5194/hess-
980 29-3037-2025
981 Gimeno, L., Drumond, A., Nieto, R., Trigo, R.M., Stohl, A., 2010. On the origin of continental precipitation. Geophys.
982 Res. Lett. 37. https://doi.org/10.1029/2010GL043712
983 Giraldo, R., Leiva, V., Castro, C., 2023. An overview of kriging and cokriging predictors for functional random fields.
984 Math. 11, 3425. https://doi.org/10.3390/math11153425
985 Gleeson, T., Cuthbert, M.O., Ferguson, G., Perrone, D., 2020. Groundwater sustainability. Nat. Geosci.
986 https://doi.org/10.1038/s41561-020-00688-8
987 Gleeson, T., Wagener, T., Döll, P., Zipper, S.C., West, C., Wada, Y., 2021a. Advancing groundwater sustainability
988 through large-scale assessment. Nat. Geosci. https://doi.org/10.1038/s41561-021-00717-6
989 Gleeson, T., Wagener, T., Döll, P., Zipper, S. C., West, C., Wada, Y., Taylor, R., Scanlon, B., Rosolem, R., Rahman, S.,
990 Oshinlaja, N., Maxwell, R., Lo, M.-H., Kim, H., Hill, M., Hartmann, A., Fogg, G., Famiglietti, J. S., Ducharne, A.,
991 de Graaf, I., Cuthbert, M., Condon, L., Bresciani, E., and Bierkens, M. F. P., 2021b. GMD perspective: The
992 quest to improve the evaluation of groundwater representation in continental- to global-scale models,
993 Geosci. Model Dev., 14, 7545–7571, https://doi.org/10.5194/gmd-14-7545-2021
994 Gong, H., Pan, Y., Zheng, L., Li, X., Zhu, L., Zhang, C., Huang, Z., Li, Z., Wang, H., Zhou, C., 2018. Long-term groundwater
995 storage changes and land subsidence development in the North China Plain (1971–2015). Hydrogeol. J. 26,
996 1417–1427. https://doi.org/10.1007/s10040-018-1768-4

Gonzalez-Hidalgo, J. C., Trullenque-Blanco, V., Beguería, S., Peña-Angulo, D., 2024. Seasonal precipitation changes in the western Mediterranean Basin: The case of the Spanish mainland, 1916-2015. Int. J. Climatol. 44(5), 1800-1815. https://doi.org/https://doi.org/10.1002/joc.8412

Goovaerts, P., 1997. Geostatistics for Natural Resources Evaluation. Oxford University Press. https://books.google.de/books?id=CW-7tHAaVR0C

Gringarten, E., Deutsch, C.V., 2001. Teacher's aide variogram interpretation and modeling. Math. Geol. https://doi.org/10.1023/A:1011097023966

Haitjema, H.M., Mitchell-Bruker, S., 2005. Are water tables a subdued replica of the topography? Ground Water 43, 781–786. https://doi.org/10.1111/j.1745-6584.2005.00090.x

Hartmann, A., Gleeson, T., Wada, Y., Wagener, T., 2017. Enhanced groundwater recharge rates and altered recharge sensitivity to climate variability through subsurface heterogeneity. Natl. Acad. Sci. U.S.A. 114(11), 2842-2847. https://doi.org/10.1073/pnas.1614941114

He, X. L., Sonnenborg, T. O., Jørgensen, F., Jensen, K. H., 2014. The effect of training image and secondary data integration with multiple-point geostatistics in groundwater modelling. Hydrol. Earth Syst. Sci. 18, 2943–2954, https://doi.org/10.5194/hess-18-2943-2014

Hellwig, J., de Graaf, I. E. M., Weiler, M., Stahl, K., 2020. Large-scale assessment of delayed groundwater responses to drought. Water Resour. Res. 56(2), e2019WR025441. https://doi.org/https://doi.org/10.1029/2019WR025441

Hengl, T., Nussbaum, M., Wright, M.N., Heuvelink, G.B.M., Gräler, B., 2018. Random forest as a generic framework for spatial prediction. PeerJ https://doi.org/10.7717/peerj.5518

Huang, Z., Pan, Y., Gong, H., Yeh, P.J.F., Li, X., Zhou, D., Zhao, W., 2015. Subregional-scale groundwater depletion detected by GRACE for both shallow and deep aquifers in the North China Plain. Geophys. Res. Lett. 42, 1791–1799. https://doi.org/10.1002/2014GL062498

Huggins, X., Gleeson, T., Serrano, D., Zipper, S., Jehn, F., Rohde, M.M., Abell, R., Vigerstol, K., Hartmann, A., 2023. Overlooked risks and opportunities in groundwater sheds of the world's protected areas. Nat. Sustain. 6 (7) 855-864. 10.1038/s41893-023-01086-9

Journel, A.G., Huijbregts, C.J., 2016. Mining Geostatistics. Academic Press.

Koch, J., Berger, H., Henriksen, H.J., Sonnenborg, T.O., 2019. Modelling of the shallow water table at high spatial resolution using random forests. Hydrol. Earth Syst. Sci. 23, 4603-4619. https://doi.org/10.5194/hess-23-4603-2019

Kumar, M., Duffy, C.J., Salvage, K.M., 2021. Evaluating groundwater controls at regional scales. Water Resour. Res. https://doi.org/10.1029/2020WR028751

Lark, R.M., 2012. Robust estimation of variograms. Comput. Geosci. https://doi.org/10.1016/j.cageo.2011.11.007

Li, Y., Fang, K., Chen, X., 2023. Auxiliary variable selection in groundwater interpolation. J. Hydrol. https://doi.org/10.1016/j.jhydrol.2023.129841

Liu, Y., Shan, F., Yue, H., Wang, X., Fan, Y., 2023. Global analysis of the correlation and propagation among meteorological, agricultural, surface water, and groundwater droughts. J. Environ. Manage. 333, 117460. https://doi.org/10.1016/j.jenvman.2023.117460

Llamas, M.R., Martínez-Santos, P., 2005. Intensive groundwater use: silent revolution and potential source of social conflicts. J. Water Resour. Plann. Manag. 131(5), 337–341. https://doi.org/10.1061/(ASCE)0733-9496(2005)131:5(337)

López-Moreno, J. I., Vicente-Serrano, S. M., Angulo-Martínez, M., Beguería, S., Kenawy, A., 2010. Trends in daily precipitation on the northeastern Iberian Peninsula, 1955-2006. Int. J. Climatol. 30(7), 1026-1041. https://doi.org/10.1002/joc.1945

Lorenzo-Lacruz, J., Garcia, C., Morán-Tejeda, E., 2017. Groundwater level responses to precipitation variability in Mediterranean insular aquifers. J. Hydrol. 552, 516-531. https://doi.org/10.1016/j.jhydrol.2017.07.011

Ma, Z., Liu, H., Mi, Z., Zhang, Z., Wang, Y., Xu, W., Jiang, L., He, J.-S., 2017. Climate warming reduces the temporal stability of plant community biomass production. Nat. Commun. 8, 15378. https://doi.org/10.1038/ncomms15378

Manna, F., Murray, S., Abbey, D., Martin, P., Cherry, J., Parker, B., 2019. Spatial and temporal variability of groundwater recharge in a sandstone aquifer in a semiarid region. Hydrol. Earth Syst. Sci. 23(4), 2187-2205. https://doi.org/10.5194/hess-23-2187-2019

Herrera, S., Cardoso, R. M., Soares, P. M., Espírito-Santo, F., Viterbo, P., and Gutiérrez, J. M., 2019. Iberia01: a new gridded dataset of daily precipitation and temperatures over Iberia, Earth Syst. Sci. Data, 11, 1947–1956, https://doi.org/10.5194/essd-11-1947-2019

Martínez-de la Torre, A., Miguez-Macho, G., 2019. Groundwater influence on soil moisture memory and land atmosphere fluxes in the Iberian Peninsula. Hydrol. Earth Syst. Sci. 23(12), 4909-4932. https://doi.org/10.5194/hess-23-4909-2019

Martín-Rodríguez, J. F., Mudarra, M., De la Torre, B., Andreo, B., 2023. Towards a better understanding of time-lags in karst aquifers by combining hydrological analysis tools and dye tracer tests. Application to a binary karst aquifer in southern Spain. J. Hydrol. 621, 129643. https://doi.org/10.1016/j.jhydrol.2023.129643

Millán, M.M., Estrela, M.J., Sanz, M.J., Mantilla, E., Martín, M., Pastor, F., Salvador, R., Vallejo, R., Alonso, L., Gangoiti, G., Ilardia, J.L., Navazo, M., Albizuri, A., Artíñano, B., Ciccioli, P., Kallos, G., Carvalho, R.A., Andrés, D., Hoff, A., Werhahn, J., Seufert, G., Versino, B., 2005. Climatic feedbacks and desertification: The Mediterranean model. J. Clim. 18, 684–701. https://doi.org/10.1175/JCLI-3283.1

Miró, J. J., Estrela, M. J., Corell, D., Gómez, I., Luna, M. Y., 2023. Precipitation and drought trends (1952–2021) in a key hydrological recharge area of the eastern Iberian Peninsula. Atmos. Res. 286, 106695. https://doi.org/10.1016/j.atmosres.2023.106695

Moench, M., Burke, J. J., Moench, Y., 2009. Rethinking the approach to groundwater and food security, Tech.Rep., Water Reports24, FAO, Rome, Italy, available at: http://www.fao.org/3/a-y4495e.pdf

1067 Moutahir, H., Bellot, P., Monjo, R., Bellot, J., Garcia, M., Touhami, I., 2017. Likely effects of climate change on
1068 groundwater availability in a Mediterranean region of Southeastern Spain. Hydrol. Process. 31(1), 161-176.
1069 https://doi.org/10.1002/hyp.10988
1070 Muhs, D., 2020. The influence of topography on the spatial variability of soils in Mediterranean climates. In (pp. 269-
1071 284). https://doi.org/10.4324/9780429297977-12
1072 Olea, R.A., 2009. Geostatistics for Engineers and Earth Scientists. Springer.
1073 Owuor, S. O., Butterbach-Bahl, K., Guzha, A. C., Rufino, M. C., Pelster, D. E., Díaz-Pinés, E., Breuer, L., 2016.
1074 Groundwater recharge rates and surface runoff response to land use and land cover changes in semi-arid
1075 environments. Ecol. Process. 5(1), 16. https://doi.org/10.1186/s13717-016-0060-6
1076 Pérez, I.A., García, MÁ., 2023. Climate change in the Iberian Peninsula by weather types and temperature. Atmos. Res.
1077 284, 106596. https://doi.org/10.1016/j.atmosres.2022.106596
1078 Portoghese, I., Matarrese, R., Mirra, L., Giannoccaro, G., 2025. Assimilating farmers' behaviour in the development of
1079 an ET-based irrigation water-accounting model. Water Resour. Manage. 39, 7749–7774.
1080 https://doi.org/10.1007/s11269-025-04316-1
1081 Power, G., Brown, RS., Imhof, J.G., 1999. Groundwater and fish insights from northern North America. Hydrol. Process.
1082 13, 401-422. https://doi.org/10.1002/(SICI)1099-1085(19990228)13:3<401::AID-HYP746>3.0.CO;2-A
1083 Rao, P., Wang, Y., Liu, Y., Wang, X., Hou, Y., Pan, S., Wang, F., Zhu, D., 2022. A comparison of multiple methods for
1084 mapping groundwater levels in the Mu Us Sandy Land, China. J. Hydrol. Reg. Stud. 43, 101189.
1085 https://doi.org/10.1016/j.ejrh.2022.101189
1086 Ravish, S., Setia, B., Deswal, S., Puri, V., Singh, B., Sharma, K., Yadav, A.K., 2025. Improving the estimation precision of
1087 the mapping of groundwater salinity by employing the indicator kriging technique. Appl. Water Sci. 15, 149.
1088 https://doi.org/10.1007/s13201-025-02512-3
1089 Refsgaard, J.C., Iversen, J.J.L., Jensen, K.H., 2021. Distributed hydrological modeling for groundwater recharge
1090 evaluation. Water Resour. Res. https://doi.org/10.1029/2020WR028271
1091 Rios-Entenza, A., Soares, P.M.M., Trigo, R.M., Cardoso, R.M., Miguez-Macho, G., 2014. Moisture recycling in the
1092 Iberian Peninsula from a regional climate simulation: Spatiotemporal analysis and impact on the precipitation
1093 regime. J. Geophys. Res. Atmos. 119, 5895-5912. https://doi.org/10.1002/2013JD021274
1094 Rodríguez-Rodríguez, L., Jiménez-Sánchez, M., Domínguez-Cuesta, M. J., Aranburu, A., 2015. Research history on
1095 glacial geomorphology and geochronology of the Cantabrian Mountains, north Iberia (43–42°N/7–2°W).
1096 Quat. Int. 364, 6-21. https://doi.org/https://doi.org/10.1016/j.quaint.2014.06.007
1097 Rohde, M.M., Albano, C.M., Huggins, X., Klausmeyer, K.R., Morton, C., Sharman, A., Zaveri, E., Saito, L., Freed, Z.,
1098 Howard, J.K., Job, N., Richter, H., Toderich, K., Rodella, A.S., Gleeson, T., Huntington, J.L., Chandanpurkar,
1099 H.A., Purdy, A.J., Famiglietti, J.S., Singer, M.B., Roberts, D.A., Caylor, K., Stella, J.C., 2024. Groundwater-
1100 dependent ecosystem map exposes global dryland protection needs. Nature 632, 101–107.
1101 https://doi.org/10.1038/s41586-024-07702-8

Rouhani, A., Ben-Salem, N., D'Oria, M., Chávez García Silva, R., Viglione, A., Copty, N.K., Rode, M., Barry, D.A., Gómez-Hernández, J.J., Jomaa, S., 2025. Direct impact of climate change on groundwater levels in the Iberian Peninsula. Sci. Total Environ. 970, 179009. https://doi.org/10.1016/j.scitotenv.2025.179009

Ruiz, M. C., Valdés-Abellán, J., Pla, C., Fernández-Mejuto, M., Benavente, D., 2023. Land Cover Changes and Their Influence on Recharge in a Mediterranean Karstic Aquifer (Alicante, Spain). Land. 12(1), 128. https://www.mdpi.com/2073-445X/12/1/128

Rusli, S.R., Bense, V.F., Mustafa, S.M.T., Weerts, A.H., 2024. Impact of climate change and groundwater abstraction on basin-scale groundwater availability. Hydrol. Earth Syst. Sci. https://doi.org/10.5194/hess-28-5107-2024

Ruybal, C.J., Sweetkind, D.S., Faunt, C.C., 2022. Regional-scale groundwater surface mapping. J. Hydrol. https://doi.org/10.1016/j.jhydrol.2022.127533

Somers, L. D., McKenzie, J. M., 2020. A review of groundwater in high mountain environments. WIREs Water. 7(6), e1475. https://doi.org/10.1002/wat2.1475

Taylor, R., Scanlon, B., Döll, P. et al. Groundwater and climate change. Nature Clim Change 3, 322–329 (2013). https://doi.org/10.1038/nclimate1744

Tularam, G.A., Keeler, H.N., 2024. Climate drivers of groundwater recharge under semi-arid to Mediterranean conditions. J. Arid Environ. https://doi.org/10.1016/j.jaridenv.2024.104505

Wackernagel, H., 2003. Multivariate geostatistics: An introduction with applications. 3rd ed. Springer, Berlin, Heidelberg. https://doi.org/10.1007/978-3-662-05294-5

Wada, Y., van Beek, L.P.H., van Kempen, C.M., Reckman, J.W.T.M., Vasak, S., Bierkens, M.F.P., 2010. Global depletion of groundwater resources. Geophys. Res. Lett. 37, L20402. https://doi.org/10.1029/2010GL044571

Webster, R., Oliver, M.A., 2007. Geostatistics for Environmental Scientists. Wiley. Xanke, J., Liesch, T., 2022. Quantification and possible causes of declining groundwater resources in the Euro-Mediterranean region from 2003 to 2020. Hydrogeol. J. 30(2), 379-400. https://doi.org/10.1007/s10040-021-02448-3

Xiao, H., Tang, Y., Li, H., Zhang, L., Ngo-Duc, T., Chen, D., Tang, Q., 2021. Saltwater intrusion into groundwater systems in the Mekong Delta and links to global change. Adv. Clim. Change Res. 12(3), 342-352. https://doi.org/https://doi.org/10.1016/j.accre.2021.04.005

Zhang, Y., Schaap, M.G., 2019. Upscaling groundwater processes in large-scale models. Water Resour. Res. https://doi.org/10.1029/2018WR024480

Zimmerman, D.L., 2006. Optimal prediction of spatial random fields. J. Stat. Plan. Inference https://doi.org/10.1016/j.jspi.2004.12.002

Zimmerman, D.L., Ver Hoef, J.M., Cressie, N., 2020. Spatial statistical modeling. Stat. Sci. https://doi.org/10.1214/19-STS746